Available online at www.sciencedirect.com
ScienceDirect
ELSEVIER
Palaeogeography, Palaeoclimatology, Palaeoecology 238 (2006) 190–218
PALAEO
www.elsevier.com/locate/palaeo

Geographic and temporal patterns in the late Neogene (12–3 Ma) aridification of Europe: The use of small mammals as paleoprecipitation proxies

Jan A. van Dam *

Utrecht University, Faculty of Earth Sciences, Budapestlaan 4, 3584 CD Utrecht, The Netherlands

Received 30 June 2003; accepted 7 March 2006

Abstract

Present-day relations between small-mammal community structure and rainfall are used to predict late Neogene (12–3 Ma) precipitation patterns in Europe and Anatolia. New proxy methods are developed which include regressions of mean annual and minimum monthly precipitation on diet (Invertivory Index) and locomotion/habitat (Arboreality Index). A series of precipitation maps and a set of regional precipitation curves through time at 1 Myr resolution are presented. Precipitation curves at a higher temporal resolution are constructed for the region of central Spain.

The Miocene results show the existence between 12 and 9 Ma of a large wet (800–1200 mm/yr) zone, extending from northern Spain to the Ukraine, and characterized by the whole-year penetration of large amounts of moisture far into the continent. Between 10–9 and 5 Ma, this European Temperate Wet Zone (ETWZ) shrinks and/or moves northward, resulting in diachronous aridification. A coeval northward migration of the Subtropical High Pressure Zone (SHPZ) is hypothesized, which is also consistent with the predicted onset of seasonal (summer) dryness between 10 and 8 Ma.

The maximum extension of the ETWZ at 12–9 Ma temporally correlates with Northern Hemisphere cooling, suggesting that climate zonation rather than the global amount of atmospheric moisture controlled European climate at this time. The main aridification at 9–8 Ma could best be explained by a northward extension/shifting of the Subtropical High Pressure Zone, and a transition towards less zonal circulation, processes which ultimately could have been triggered by uplift of the Tibetan plateau. A temporary increase of precipitation at 7–6 Ma is associated with renewed global cooling. The lowest precipitation values (less than 400 mm/yr) occur during the Pliocene in Southern and Eastern Europe. Uplift in Eastern Europe (Carpathians, shrinking of the Paratethys) could well explain the aridification in this area and the associated sharpening of east–west precipitation gradients across the continent.

Keywords: Precipitation; Climate; Seasonality; Mammals; Miocene; Pliocene; Europe

1. Introduction

The late Neogene represents a significant episode in Cenozoic climatic history. It is during this interval that continents witness a major expansion of dry zones, and that forests are replaced by woodlands and grasslands, particularly in the mid-latitudes (Crowley and North, 1991; Potts and Behrensmeyer, 1992). The ultimate cause(s) of this global aridification are not yet fully understood, although it is commonly believed that there is a general relation with global Cenozoic cooling.

* Fax: +31 30 2532648.
E-mail address: jdam@geo.uu.nl.

0031-0182/$ - see front matter © 2006 Elsevier B.V. All rights reserved.
doi:10.1016/j.palaeo.2006.03.025

Because atmospheric moisture content decreases with decreasing air temperature it is to be expected that global cooling should somehow lead to net aridification on the planet. Cooling and aridification trends do not seem to run parallel, however. For example major aridification and expansion of open environments occurred during the Late Miocene (11.2–5.3 Ma), as evidenced by the appearance of four new open-land, arid-adapted vegetation families (Singh, 1988). However, only "minor" cooling steps around 10 Ma and between 5.5 and 5 Ma have been documented, and it is generally believed that the two most important Late Cenozoic global cooling steps occurred earlier, during the Middle Miocene (14 Ma) and later, at 2.5 Ma (Frakes et al., 1992; Zachos et al., 2001). Evidently, other factors than temperature have strong effects on precipitation regimes as well, particularly paleotopography and continental configuration by affecting ocean currents and continentality. In addition, the spatial complexity of the systems of atmospheric and oceanic circulation ensures that general cooling may result in precipitation decrease in some regions and increase in others.

The well-documented terrestrial floral and faunal record of Europe (and Anatolia) provides an excellent case for the study of trends and gradients in late Neogene aridification. It is clear that the trend was not straightforward and simple. For instance, the palynological and paleobotanical record shows drying at different times in different areas, e.g. in Bulgaria around 11 Ma (Ivanov et al., 2002) and SW central France around 9 Ma (Farjanel and Mein, 1984). On the other hand, precipitation estimates on the basis of floras from Northern Germany remain at high levels throughout the Late Miocene, to drop only during the Early Pliocene (Utescher et al., 2000). Similarly, pollen records on Sicily do not indicate any significant humidity change or aridification between the Late Tortonian (Middle late Miocene) and lower Zanclean (Early Pliocene) (Suc and Bessais, 1990). The rich European mammal record clearly indicates the establishment of a drier climate during the late Neogene. Grassland/woodland-adapted bovids and horses start to dominate the Mediterranean assemblages during the early Late Miocene, with dietary and locomotor spectra indicating open-country environments (Fortelius et al., 1996). A coeval rise is noted in average large-mammal hypsodonty, a measure that correlates positively with aridity (Damuth and Fortelius, 2001; Fortelius et al., 2002). Around 10–9 Ma ("Vallesian crisis") the distribution areas of many forest-adapted forms are strongly reduced and some groups, such as the hominoids, disappear from Europe all together (Andrews and Bernor, 1999; Fortelius and Hokkanen, 2001).

The small-mammal record indicates aridification as well. For example the rodent record from central Spain indicates a major trend towards more dry conditions and wet–dry seasonality between 9.5 and 8 Ma, resulting in a sharper north–south gradient towards central Europe (van Dam and Weltje, 1999). The present paper can be regarded as a follow-up to this study, from which it differs by its wider geographic and temporal coverage, its use of complete small-mammal faunas instead of rodent assemblages only, its more direct taxon-free approach, and its use of richness instead of abundance. Richness data are chosen because they allow a direct calibration to present-day precipitation levels.

Present-day European mean annual precipitation shows distinct east–west and north–south gradients. The eastward trend of decreasing precipitation reflects increasing continentality towards the Asian interior. The northward gradient reflects the transition from the subtropical–dry belt (Sahara and Middle East deserts) to the temperate humid belt of central–northern Europe. The area of summer dryness is situated in between, over the Mediterranean region (Fig. 1). Seasonality of precipitation has major effects on vegetation and faunal structure in this region, because the presence of a distinct dry season results in open landscapes in spite of a high annual amount of rain. For this reason, not only mean annual precipitation, but also the seasonal distribution of rainfall will be addressed in this paper.

2. Small mammals as paleoprecipitation proxies

Paleoprecipitation proxies are relatively rare. This is not only a handicap for climatic reconstructions, but also for climatic modeling, especially because the modeling of precipitation is more complicated than that of temperature (Ruddiman et al., 1997). Among the successfully used abiotic proxies are the distribution of evaporites and coals (Parrish et al., 1982), lake levels (e.g. Nicholson and Flohn, 1980) and the presence and depth of pedogenic calcium carbonate (Retallack, 2000b). Most biotic proxies or proxy methods are based on palynological and paleobotanical data. For example, recently developed methods combining individual climatic requirements from still living and related forms have proved to be successful in predicting late Neogene precipitation levels (Mosbrugger and Utescher, 1997; Fauquette et al., 1998). Terrestrial invertebrates (e.g. fresh-water gastropods) and lower vertebrates indicate the presence of water bodies and humid conditions and can be used to infer relative trends in precipitation (Böhme, 2003).

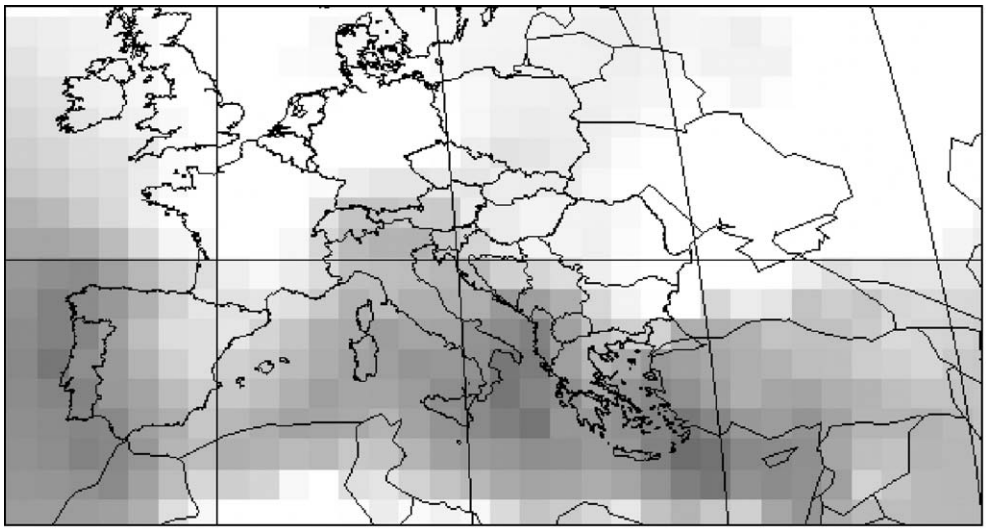

Fig. 1. Present-day distribution of seasonality of precipitation (SEASP). SEASP is calculated as the difference between 30-year means of MAXP (precipitation in the wettest month) and MINP (precipitation in the driest month). Data from Müller (1996) and KNMI (1997). Darker colors indicate larger seasonality. See caption of Fig. 9 for details on the spatial interpolation method.

Terrestrial mammal fossils are relatively common in continental sediments. In contrast to plants, they may preserve well under dry conditions. In addition their biostratigraphic value is high. On the other hand, the extrapolation of climatic tolerance ranges from modern to fossil forms is less straightforward than in the case of plants, because many late Neogene mammal species and genera have disappeared. Genus extinction rates of mammals exceed those of plants, of which all modern genera were essentially present by the early Late Miocene (Traverse, 1982). For this reason mammal paleoecologists more and more revert to "taxon-free" methods, which use ecological classifications and ecomorphology across communities (Damuth, 1992).

The data used in this paper consist of samples of isolated small-mammal teeth (which can be regarded as the "pollen" of mammal paleontology). These samples generally reflect very well the original communities, with both the species composition and relative abundances showing good temporal and spatial persistency.

Various ecological categories of small mammals are expected to display a significant relation to precipitation. Especially good candidates are the arboreal and insectivorous categories. The presence of primary consumers with a arboreal feeding habitat and/or locomotion (e.g. flying and tree squirrels, arboreal dormice) is dependent on the productivity and complexity of the vegetation, which are, in turn, largely dependent on precipitation (Kay and Madden, 1997). As secondary consumers, insectivorous species profit from the abundance of insects and other small invertebrates in moist environments such as forests and humid soils, and hence are dependent on precipitation as well. In addition, small-sized insectivores such as shrews display high metabolic rates, resulting in high water loss and overheating in warm and dry areas (Reumer, 1985; Churchfield, 1990).

3. Present-day relationships

3.1. The locality level

As a first step, present-day relationships between precipitation and small-mammal community structure were studied. The area of analysis comprises the northwestern part of the Old World, i.e. Europe, North Africa and the Middle East, with the southern boundary at 20°N and the eastern boundary at 60°E. The units of analysis represent local, relatively undisturbed habitats such as nature reserves and national parks (Table 1, Fig. 2), for which species lists, vegetation types, and climatic parameters have been compiled (Damuth, 1999; Badgley, pers. comm.). Vegetation types include desert (including semi-desert), woodland (Mediterranean vegetation), and temperate forest. Included orders are Lipotyphla ("Insectivora"), Lagomorpha (hares and rabbits) and Rodentia (rodents). Assignments to ecological categories (diet, feeding habitat) were based on literature data (Niethammer and Krapp, 1978; Nowak, 1991; Mitchell-Jones et al., 1999). The analysis was restricted terrestrial species sensu lato: i.e. arboreal and fossorial species included. (Semi)aquatic taxa (*Neomys*, *Castor*, *Arvicola*, *Ondatra*, *Myocastor*) were left out,

Table 1
Geographic, precipitation and richness data for the present-day localities used

	Locality	Country	Vegetation type	Area	Elev.	Lat.	Long.	MAP	MINP	MAXP	SEASP	NI	NA	NS	N	PI	PA	PS
				km^2	m	°N	°E	mm/yr	mm/yr	mm/yr	mm/yr					%	%	%
1	Dalsland	Sweden	Temperate forest	4100	100	58.8	12.0	666	32	83	51	4	1	2	11	36	9	18
2	Bialowieza	Poland	Temperate forest	1000	130	52.7	23.7	594	30	80	50	6	4	4	23	26	17	17
3	Trzebnickie Hills	Poland	Temperate forest	900	300	51.4	17.3	601	30	87	57	6	1	3	20	30	5	15
4	Cesky Les	Czech Rep.	Temperate forest	1000	400	49.8	13.6	514	22	75	53	7	3	5	22	32	14	23
5	Biesczady Mts	Poland	Temperate forest	1000	900	49.5	22.4	708	33	99	66	7	4	5	21	33	19	24
6	Nowy Targ Valley	Poland	Temperate forest	1200	500	49.5	20.0	886	43	128	85	7	4	5	23	30	17	22
7	Tatras	Poland	Temperate forest	200	1200	49.5	20.0	744	36	95	59	6	3	4	20	30	15	20
8	Rhone Valley	France	Temperate forest	1000	150	44.8	4.0	813	46	93	47	10	4	7	29	34	14	24
9	Terek–Kuma Sector	Russia	Desert	10,000	0	44.3	46.3	344	14	54	40	4	0	2	20	20	0	10
10	Doñana	Spain	Woodland	100	50	37.0	−6.5	535	1	84	83	3	0	2	8	38	0	25
11	Algiers	Algeria	Woodland	2500	60	36.8	3.0	691	2	117	115	3	0	2	13	23	0	15
12	Aghbolagh Morched	Iran	Desert	400	1300	35.7	46.5	443	0	79	79	2	0	1	14	14	0	7
13	Biskra	Algeria	Desert	2500	125	34.8	5.7	129	0	19	19	4	0	2	20	20	0	10
14	Lebanon	Lebanon	Woodland	10,400	1000	33.8	35.9	615	1	157	156	4	2	2	20	20	10	10
15	Azraq	Jordan	Desert	5250	520	31.9	36.8	74	0	18	18	4	0	2	19	21	0	11
16	Shush	Iran	Desert	10,000	80	31.0	48.5	196	0	46	46	1	0	0	15	7	0	0
17	El Golea	Algeria	Desert	2500	400	30.5	2.8	56	1	13	12	1	0	0	11	9	0	0
18	Beni Abbes	Algeria	Desert	2500	500	30.2	−2.2	90	0	14	14	1	0	0	13	8	0	0
19	Kuwait	Kuwait	Desert	17,818	150	29.0	47.5	122	0	31	31	2	0	0	11	18	0	0
20	United Arab Emirates	Un. Ar. Em.	Desert	92,100	150	24.0	54.0	77	0	32	32	2	0	0	10	20	0	0
21	Tamanrassett	Algeria	Desert	10,000	1380	22.7	5.5	42	1	10	9	1	0	0	12	8	0	0

For further explanation of precipitation and richness variables: see Tables 2 and 3.

because the presence of a particular permanent water body may be dependent on other factors as well (tectonics) and might not represent the regional rainfall gradient. Aerial species (Chiroptera, bats) were excluded because of their under-representation in the fossil record. Commensal terrestrial species (*Mus musculus*, *Rattus rattus*, *Rattus norvegicus*) were left out as well.

Four rainfall variables were considered: mean annual precipitation (MAP), precipitation in the driest month (= minimum monthly rainfall) (MINP), precipitation in the wettest month (= maximum monthly rainfall) (MAXP), and seasonality of precipitation (SEASP), which is calculated as the difference of MAXP and MINP. The correlations for the data set (Table 2) show that MAP and MAXP are highly correlated, but that both show lower (but still significant) correlations to MINP. These lower correlations with MINP are mainly due to the inclusion of the Mediterranean localities, which have highly seasonal regimes (e.g. Algiers in N Africa, Doñana in S Spain, and Lebanon in the Middle East) characterized by high mean and maximum levels but with almost no rainfall in the driest months (Fig. 1). SEASP shows a higher correlation with MAXP than with MINP, because MINP values are constrained at the lower end (no rain).

Because of their expected relationship to rainfall (see above), arboreality and invertivory were selected as the key properties for precipitation prediction. By "arboreal" I mean here: with an arboreal feeding habitat or with arboreal or scansorial locomotion (see Damuth (1992) for terminology and classification). "Invertivore" is used instead of "insectivore", because predation of tiny animal prey usually involves both insects and non-insect invertebrates (spiders, earthworms, gastropods, etc., see Badgley and Fox, 2000). Both the absolute numbers and proportions of species were analyzed, resulting in the four variables NA, NI, PA and PI (Table 3). The

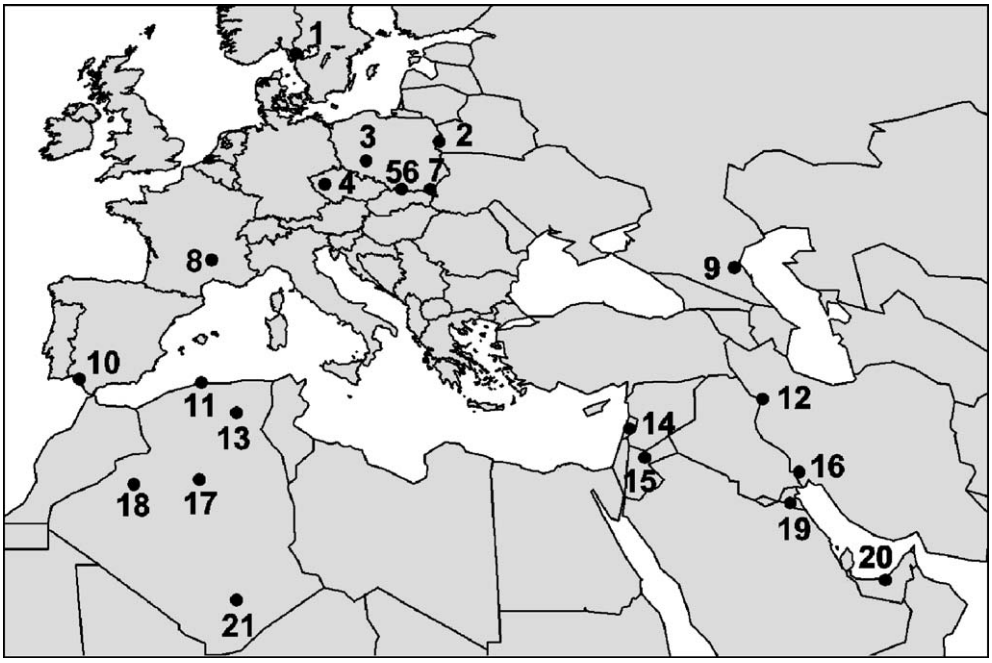

Fig. 2. Recent mammal localities used in this study. Faunal lists and rainfall values are from Badgley (pers. comm.) and included in a data base of the Working Group on "Climatic and Habitat Inference from Mammalian Communities" at the National Center of Ecological Analysis and Synthesis (NCEAS), University of California, Santa Barbara (Damuth, 1999). 1. Dalsland, 2. Bialowieza, 3. Trzebnickie Hills, 4. Cesky Les, 5. Biesczady Mountains, 6. Nowy Targ Valley, 7. Tatras, 8. Rhone Valley, 9. Terek–Kuma Sector, 10. Doñana, 11. Algiers, 12. Aghbolagh Morched, 13. Biskra, 14. Lebanon, 15. Azraq, 16. Shush, 17. El Golea, 18. Beni Abbes, 19. Kuwait, 20. United Arabian Emirates, and 21. Tamanrassett.

percentage PA is comparable to the "Arboreality Index" defined by Kay and Madden (1997), which is used for paleoprecipitation estimations for the Middle Miocene of South America on the basis of small and large mammals together. Variables comparable to PA and PI have also been used in ecological diversity spectra that were used for vegetation reconstructions (Andrews et al., 1979). Here, PI will be referred to as "Invertivory Index".

Because total diversity is an important community variable as such, the total number of species (*N*) was considered as well. A disadvantage of applying total species richness to the fossil record is the requirement of a more or less complete sampling of the fossil localities or at least a comparable degree of sampling for recent and fossil localities. The use of indices such as PA and PI is less problematic, because of the less restrictive assumption that the chance of finding an additional species with increasing sampling effort is independent of its membership to a certain ecological category (arboreal versus non-arboreal, invertivore versus non-invertivore).

The values for the precipitation and faunal variables are given in Table 1. Table 4 shows simple linear

Table 2
Precipitation variables and Pearson's correlation coefficients for present-day European localities (Table 1)

Code	Precipitation variable (mm)	MAP	MINP	MAXP
MAP	Mean annual precipitation			
MMP	Mean monthly precipitation = MAP/12			
MINP	Precipitation in the driest month	**0.83**		
MAXP	Precipitation in the wettest month	**0.97**	**0.7**	
SEASP	Seasonality = MAXP − MINP	**0.78**	0.32	**0.9**
SEASL	Seasonality (lower part) = MMP − MINP			

Bold values are significant (0.01 level).

Table 3
Faunal variables and codes used

Code	Variable	Meaning
N	Species richness	Total number of species
NA	Arboreality Richness	Number of arboreal species
PA	Arboreality Index	Percentage arboreal species
NI	Invertivory Richness	Number of invertivore species
PI	Invertivory Index	Percentage invertivore species

Included orders are Lipotyphla, Lagomorpha and Rodentia. Aerial forms (Chiroptera) and (semi)aquatic species are excluded. By "arboreal" is meant: with an arboreal or canopy feeding habitat or with arboreal or scansorial locomotion (see Damuth (1992) for specific terminology). "Invertivore" is used instead of "insectivore", because many diets consist of both insects and non-insect invertebrate prey (spiders, earthworms, mollusks, etc.).

Table 4
Simple regression results with precipitation variables as independent variables and richness variables as dependent variables for modern localities

Independent variables	Dependent variable: MAP			Independent variables	Dependent variable: MINP		
	a	*b*	R^2		*a*	*b*	R^2
N	−38.712	27.472	0.24	N	2.090	−21.425	0.43
NA	129.137	265.807	0.54	NA	8.681	3.157	0.71
NI	87.972	69.613	0.56	NI	5.915	−10.037	0.74
PA	29.981	253.867	0.56	PA	1.978	2.567	0.72
PI	22.775	−93.141	0.57	PI	1.237	−14.281	0.48
Independent variables	Dependent variable: MAXP			Independent variables	Dependent variable: MAXP (excl. Lebanon)		
	a	*b*	R^2		*a*	*b*	R^2
N	3.090	15.097	0.12 *	N	2.659	18.314	0.12 *
NA	15.109	48.632	0.33	NA	13.976	46.084	0.38
NI	9.497	28.898	0.29	NI	9.533	24.246	0.40
PA	3.578	46.831	0.37	PA	3.266	44.835	0.40
PI	8.846	2.568	0.33	PI	2.716	0.609	0.51

* Not significant at the 0.05 level.

regression results, whereas Table 5 shows results of stepwise regressions. Bivariate plots and fits are shown in Figs. 3 and 4. Most of the simple linear regressions of rainfall on fauna are significant (Table 4). Only the relationships with total diversity are weak (Fig. 3). The relationships between mean annual precipitation (MAP) and the other variables are characterized by moderately strong fits (R^2=0.54–0.57, p<0.001). The shape of the point cloud is different for invertivory and arboreality: it is more or less elliptical for invertivory (Fig. 3g, j), reflecting a bivariate normal distribution, and more stepwise for arboreality (Fig. 4a, d). The stepwise pattern is caused by some high MAP values at zero values of percentage arboreality in highly seasonal regimes, such as in Algiers (North Africa) and Doñana (southern Spain) (A and D in Figs. 3 and 4). The dry summer in these areas leads to the presence of woodland instead of forest resulting in the absence of arboreal species. This observation is consistent with a better fit of NA and PA with MINP.

The strength of the relations with MAP and MINP is reversed in the case of PI. This variable correlates somewhat stronger to MAP (Fig. 4j) than to MINP (Fig. 4k). Doñana (D) is an important outlier in the plot of MINP against PI (right below in Fig. 4k). It is characterized by a high percentage of invertivores at almost zero MINP. It is known that some insectivores can survive a significantly dry season. Invertebrate prey is available even during the dry months, which is related to the whole-year availability of Mediterranean (xerophytic) evergreen vegetation as a food source. Hedgehogs and some shrew species (dry-adapted Crocidurinae) may even lower their metabolic rates and go into short periods of torpor when subjected to food shortage (Churchfield, 1990). Despite the dry summer conditions, the Mediterranean shrew and hedgehog populations are known to peak in that season (Blanco, 1998).

The fit (R^2) with MAP increases from 0.57 to 0.62 when only shrews are considered instead of invertivores as a whole. However, such a restriction is not in line with a taxon-free paleoecological approach, and is likely to introduce historical artifacts. Firstly, the use of a more general ecological category such as invertivory allows the inclusion of extinct groups (e.g. Dimylidae) and

Table 5
Stepwise regression results with precipitation variables as independent variables and richness variables as dependent variables for modern localities

	Input variables	Localities included	Equation	R^2	Range 95% CI* for observed data points
(1)	N, NA, NI, PA, PI	All	MAP=0.179+14.134* PI+18.066* PA	0.69	±350–400
(2)	N, NA, NI, PA, PI	All	MINP=−5.907+3.452* NI+1.019* PA	0.80	±17–19
(3)	PA, PI	All	MINP=2.567+1.978* PA	0.72	±19–21
(4)	N, NA, NI, PA, PI	All	MAXP=46.831+3.578* PA	0.37	±71–77
(5)	N, NA, NI, PA, PI	All, except Lebanon	MAXP=0.609+2.716* PI	0.51	±57–60

*CI = one side of two-sided confidence interval for individual locality prediction.

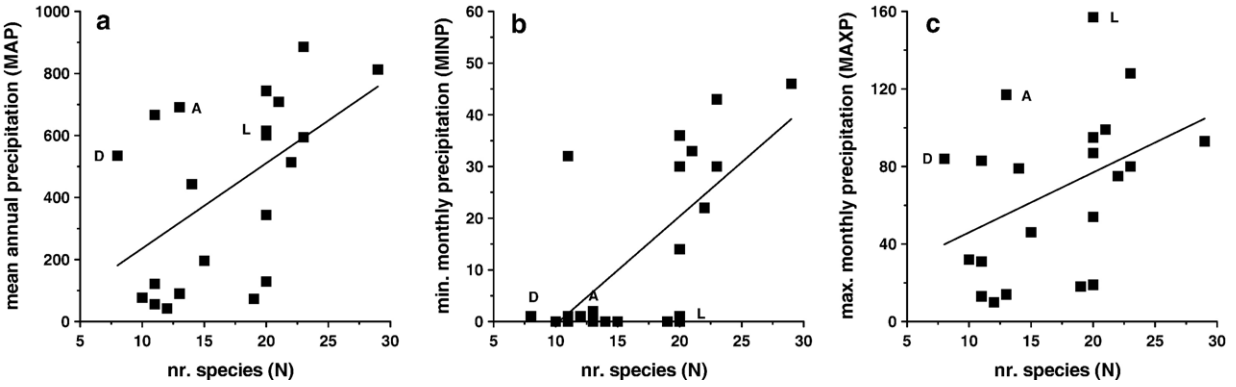

Fig. 3. Scatter plots and regressions of precipitation variables against total species richness. Mediterranean woodland localities are labeled: A = Algiers; D = Doñana; L = Lebanon.

even rodents into this category. Secondly, representatives of certain Neogene families may have filled ecological niches, which are currently occupied by members of other families. For example, Neogene hedgehogs were not dominated by Erinaceinae, but by the smaller-sized Galericinae (moon rats), which might have possessed different ecological requirements. Similarly, Uropsilinae (Talpidae), which were widespread during the late Neogene, were ecologically probably more similar to Soricidae than to Talpidae (Storch and Dahlmann, 2000).

The fits for MAXP are heavily influenced by the extreme position of the locality Lebanon (Fig. 4). This locality shows a very high value of precipitation in the wettest month, caused by its coast-nearby position in combination with an orographic effect. The apparent imbalance between MAXP and the fauna could be attributed to the locality's position in a relatively isolated small strip of seasonally humid land close to an otherwise dry (desertic) region, and a weak control by the regional species pools. When Lebanon is removed from the analysis (Table 4), R^2 values (0.41–0.51) remain rather low, however.

Stepwise regressions for MAP and MAXP result in equations, which only contain the two indices (PA, PI, Table 5). MAP can best be predicted by a multiple regression on both PA and PI, thereby raising R^2 from 0.56–0.57 (Table 4) to 0.69. b is estimated to be about zero, implying that the minimum possible MAP value would be 0 mm/yr in the absence of any arboreal or insectivorous species. The use of percentages implies a theoretical maximum value of 3220 mm/yr in case all taxa would be arboreal insectivores. A value of 1610 mm/yr is reached when 50% of the fauna is arboreal and 50% is invertivore. Such a fauna is highly theoretical as well, because some niche with terrestrial plant-eating small mammals will normally be there. Estimations on the basis of plants (see Section 4.3) suggest, however, that values above 1300 mm/yr were very rare in the late Neogene of Europe.

The best-fitting equation for MINP includes NI and PA. Because of the problem concerning the use of species richness variables (N, NA, NI) discussed above, I use the next-best fit, which is a simple regression on PA (Table 4). This results in a lowest possible value for the predicted MINP of 2.5 mm/yr, which is close to the lowest possible and observed value of 0 mm/yr. The theoretical maximum for MINP is 200 mm in the unrealistic case of 100% arboreal species.

The stepwise regression for MAXP results in a best fit with PI ($R^2 = 0.51$) (Lebanon excluded, see also Table 4). A relation of MAXP with PI is to be expected given the better fit of PI to MAP than to MINP. Nonetheless, the fit with MAXP is relatively poor. For this reason, I will restrict myself to the prediction of MAP and MINP only. An alternative seasonality measure (SEASL, the lower part of SEAS) is calculated as MMP − MINP with MMP = MAP/12.

Additional information on the MAP predictions is shown in Fig. 5. Fig. 5a shows the positive relation between PA and PI ($r = 0.64$, $p = 0.002$). Plots of MAP against predicted values and residuals are shown in Fig. 5b–c.

3.2. The grid level

A recent compilation of 50 by 50 km UTM grid-based occurrences of European mammals (Mitchell-Jones et al., 1999) was used to check the locality-level results. The data set lacks the truly arid regions of northern Africa and the Middle East, but contains northern Europe, which is represented by one locality only in the locality data set (see Section 3.1). Despite the different nature of the grid data (more human influence,

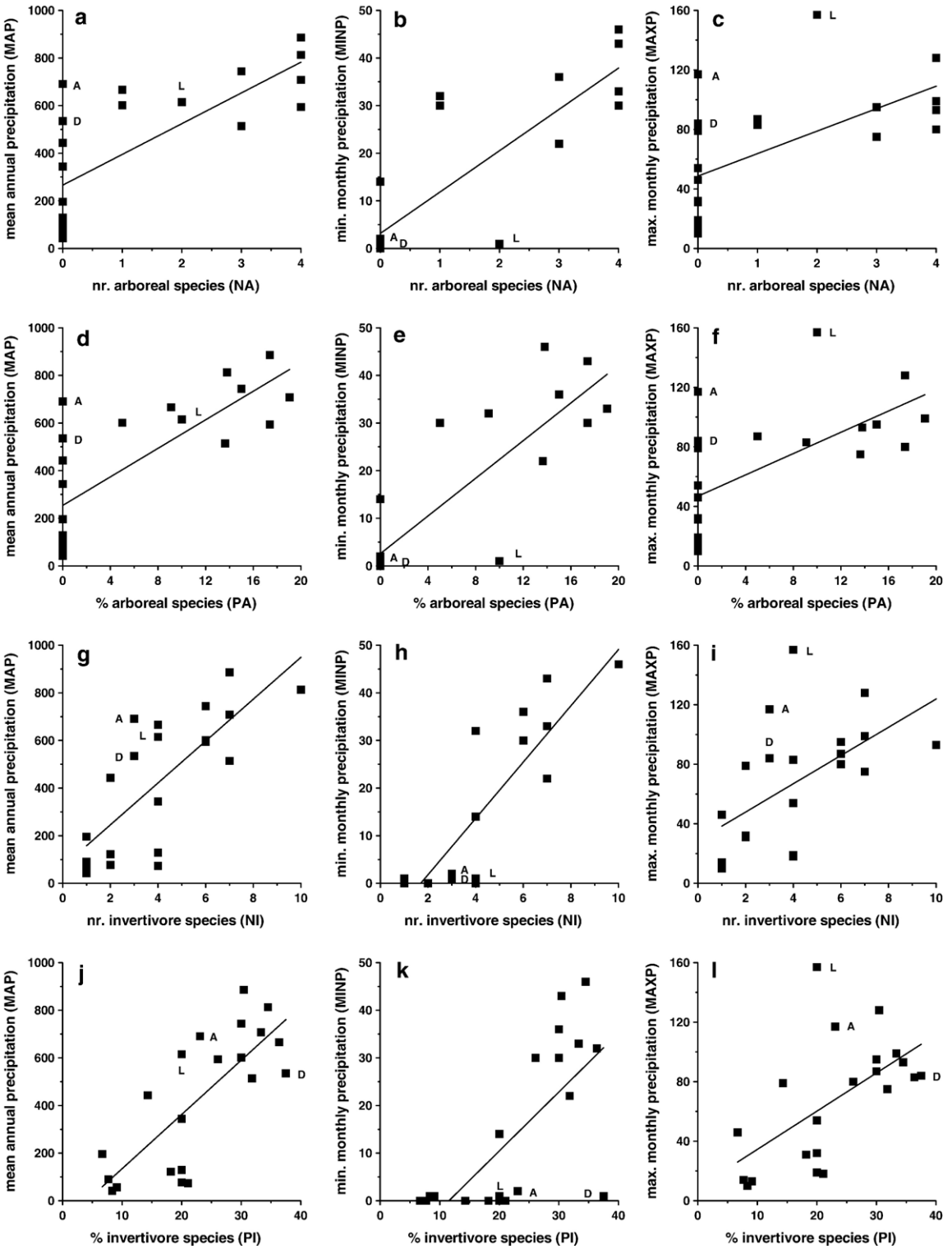

Fig. 4. Scatter plots and regressions of precipitation variables against Arboreality Richness, Arboreality Index, Invertivory Richness, and Invertivory Index. Mediterranean woodland localities are labeled: A = Algiers; D = Doñana; L = Lebanon.

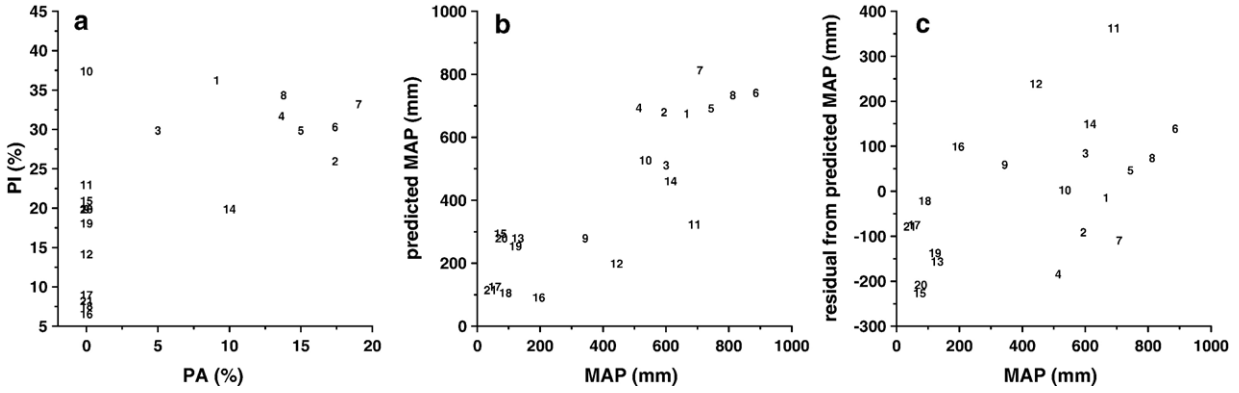

Fig. 5. Additional plots for modern localities. (a) Scatter of PI against PA, (b) scatter of predicted MAP against MAP (Table 5: Eq. (1)), (c) Scatter of residuals from predicted MAP against MAP. Labels correspond to the numbers in Table 1.

more heterogeneity), the overall patterns for central–southern Europe should be more or less consistent. Because the absence of a particular species in a grid cell can mean both absence or low sampling or observation effort (Mitchell-Jones et al., 1999), I aggregated the cells into larger units of 25 cells (62,500 km^2 large) (Fig. 6) and re-counted the species numbers in these larger units. (Semi)aquatic, aerial and commensal species were left out as was done in Section 3.1. A number of recently human-introduced forms were excluded as well (*Sylvilagus floridanus*, *Sciurus carolinensis*, *Callosciurus erythraceus*, *Callosciurus finlaysonii*). For each of the new grid cells, a representative meteorological station (Müller, 1996; KNMI, 1998) was selected.

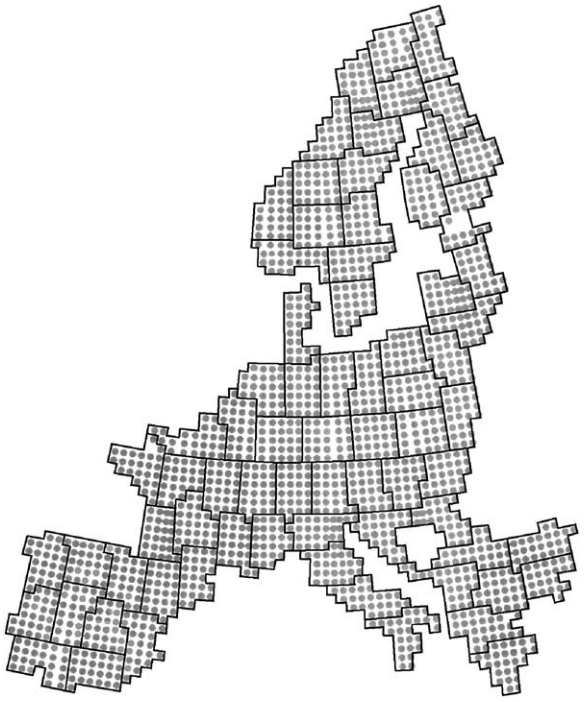

Fig. 6. Aggregated grid cells used in this paper. Each grid cell consists of 25 grid cells (50 by 50 km^2) as defined by Mitchell-Jones et al. (1999). Areas with very poor data (Rumania, Serbia) and islands are excluded.

The resulting bivariate plots are shown in Fig. 7. Grid cells with rainfall of dominantly orographic origin (e.g. Norwegian and Adriatic coasts, Alps) are indicated by a separate symbol and generally plot as outliers. This is not surprising, because equilibrium between faunal structure and precipitation levels cannot be expected for such localized areas. Northern Europe and central–southern Europe are represented by separate symbols (boundary at 50°N). A number of cells are labeled and will be discussed separately below. Generally, the results of the grid-based arboreality plots (Fig. 7a, d) are consistent with the locality-based plots (Fig. 4d, e). Because the grid data set does not include data from (semi-)deserts, the lower-left parts of Fig. 7d–e remain empty. The southern and central parts of the Iberian Peninsula show the lowest values. Two grid cells (stations Coimbra, C, and Faro, F) plot on the *Y*-axis because they do not contain a single arboreal species. The position of these cells in Fig. 7a and d is comparable to the position of Doñana and Algiers in the locality-based plots of Fig. 4d and g.

Fig 7d shows a huge variability of driest-month rainfall values at high percentages of arboreal species. This variation is caused by heterogeneous conditions within grid cells and by local rainfall anomalies. The high value of 20% arboreality in the grid cell Patras (P, most southern station in Greece), results from the contribution of only two of the 25 constituting 50 by 50 km^2 cells, and corresponds to the most seasonal rainfall regime in the data set (1 mm in the driest month,

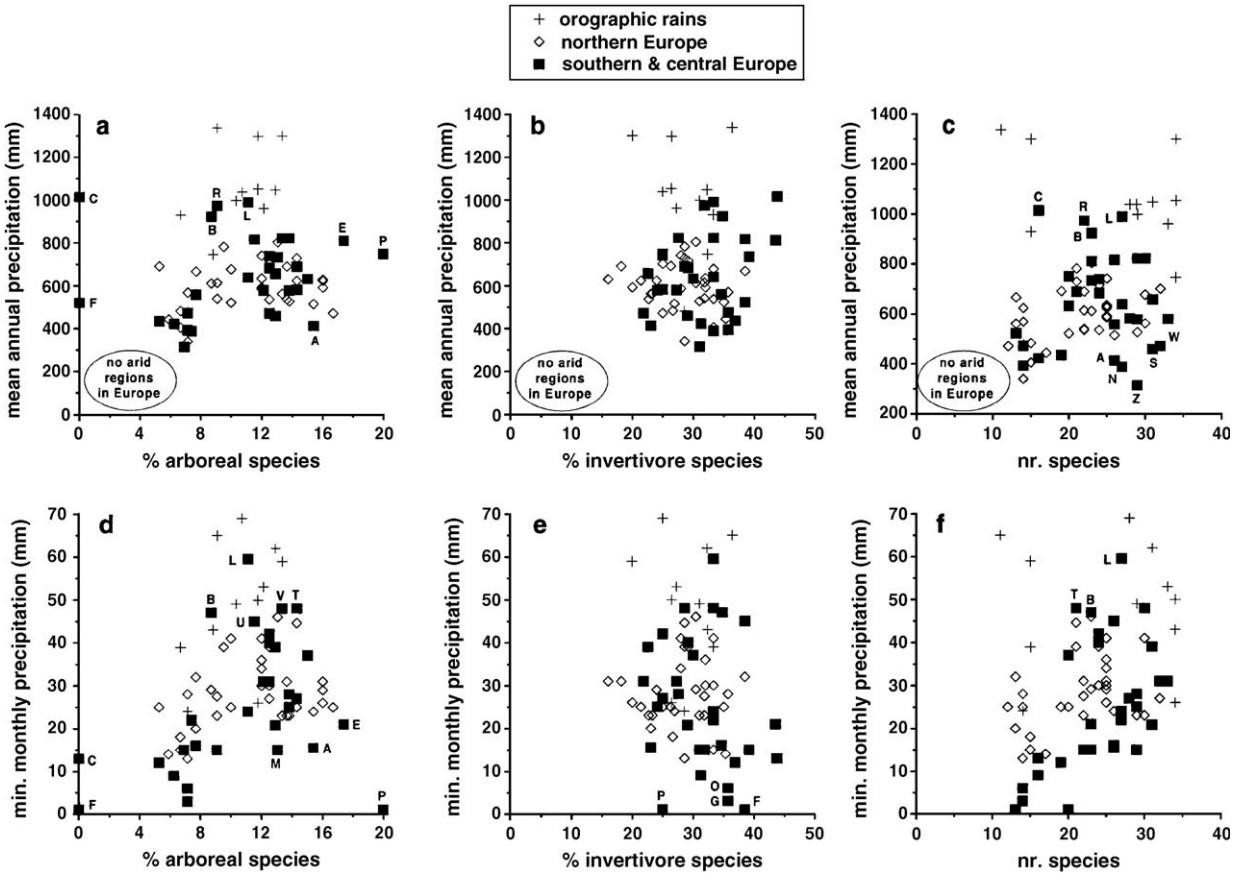

Fig. 7. Scatter plots and regressions of precipitation variables (MAP, MINP) against the Arboreality Index, Invertivory Index and total species richness. The following localities are labeled and discussed in the text: A. Larissa (C Greece), B. Bordeaux (SW France), C. Coimbra (W Iberia), E. Cosenza (S Italy), F. Faro (SW Iberia), G. Granada (S Iberia), L. Limoges (SW France), M. Rome (C Italy), N. Logroño (N Iberia), O. Los Llanos (SE Iberia), P. Patras (S Greece), R. Braganca, S. Saloniki (N Greece), U. Perugia (C Italy), V. Verona (N Italy), W. Varna (E Bulgaria), Z. Zaragoza (NE Iberia).

148 mm in the wettest month). The other southernmost eastern European grid cells (stations Larissa (A), S. Greece, and Rome (M) and Cosenza (E), Italy) also show relatively low minimum monthly rainfall levels for their arboreality indices. However, there is more reason to suspect that several localities in the top part of the figure have "too high" values: high summer rainfall at Perugia (U) and Verona (V) can be explained by their transitional positions with regard to the alpine orographic regimes in the north. The three southwestern French grids (Bordeaux, Limoges, Tours; B, L, and T) contain two or three arboreal species. These are low numbers, given the presence of forests and relatively high summer precipitation. Bordeaux and Limoges also figure as outliers in the mean annual precipitation plot (Fig. 7a) and total diversity plot (Fig. 7f), as do Braganca and Coimbra (R, C, western Iberia). These areas are all situated closely to the Atlantic coast and receive large amounts of rain. Just as in the case of orographic rains, these areas of high rainfall might be too small to carry more species. Finally, it should be noted that the lower part of Fig. 7c contains a number of grid cells with high diversities and low mean annual precipitation. Some of the high diversities, e.g. in Zaragoza (Z) and Logroño (N) may be a consequence of mixing different habitats (lowlands and mountains).

Although the plots against invertivory (Fig. 7b, e) show a different point cloud shape compared to the plots based on the locality data (Fig. 4h, k), they are basically consistent: only because the grid data set does not include the truly arid regions of Africa and the Middle East, the left-lower parts of Fig. 7b and e are empty. The lower part of Fig. 7e (minimum monthly precipitation plot), with Faro (F), Granada (G) and Los Llanos (O) (all southern Spain) and Patras (P) (southern Greece) corresponds to the part with the localities Doñana (southern Spain), and Algiers (northern Africa) in Fig. 4k, representing the seasonally-dry Mediterranean

regime. The north European point cloud (open diamonds) almost totally overlaps with the C–S European cloud except for some points with low (<20%) percentages of invertivores. The low values represent the Baltic States area. It is unclear why low proportions occur there.

The grid-level results are basically in agreement with the locality-level results. They also show clearly that the precipitation–fauna relationships may be locally "disturbed". This is especially the case in mountainous ranges, along western borders of the continent, and in mixed habitats.

4. Application: the late Neogene of Europe

4.1. Prediction uncertainties and quality of the data

The statistical uncertainty (95% confidence interval) for the predicted MAP of a locality amounts 350–400 mm/yr to either side of the mean (Table 5). Part of the noise is due to the fact that the mammal localities and the meteorological stations do not have the same geographical position. Noise is also generated by incomplete sampling, and sampling at different times. Furthermore, additional variation is introduced by using discrete species numbers resulting in discontinuous percentage "steps". Finally, there is unexplained variation due to other factors (topography, geography and other local variables). It can be argued that the prediction uncertainties for fossil localities are smaller (perhaps in the order ±200 mm) compared to the uncertainties associated with the modern localities. Human influence and the post-glacial disequilibrium have undoubtedly negatively affected the signal to noise ratio of the present-day faunal structure–precipitation relationships. Neogene landscape gradients were probably smoother, less interrupted and more stable than they are nowadays.

4.2. Ecological assignments of the fossil taxa

The following Late Miocene–Pliocene forms were assumed to be (semi)aquatic, and excluded from the analysis: Desmaninae, *Asoriculus* (Neomyini, Soricidae) and Castoridae. Also the arvicoline lineages *Mimomys hassiacus – polonicus – pliocaenicus – ostramosensis – savini*, *Dolomys nehringi – milleri*, and *Kislangia* (from Spain) were considered to be (semi) aquatic and excluded (Tesakov, 1998; Tesakov, pers. comm.; Maul, pers. comm.).

Petauristinae (flying squirrels), part of the Gliridae (dormice) and part of the extinct family Eomyidae were classified as arboreal. Extant dominantly arboreal-adapted glirid genera (*Muscardinus*, *Glis*) and extinct genera with seven or more transverse ridges in the M12 were characterized as arboreal (van der Meulen and de Bruijn, 1982; de Bruijn, 1997). As a consequence, all Myomiminae (containing the recent terrestrial genus *Myomimus*) except *Ramys* and *Vasseuromys*, and all Dryomyinae (containing the recent largely terrestrial genus *Eliomys*) except *Microdyromys complicatus*, *koenigswaldi* and *praemurinus* were classified as terrestrial sensu stricto. Feeding habitat and locomotor type of the extinct Eomyidae are not well known. It has been demonstrated that at least one Oligocene species was a glider (Storch et al., 1996), but probably not all eomyids were (Engesser, 1999). I have classified Neogene forms with five or more transverse ridges (*Pseudotheridomys*, *Eomyodon*, *Keramidomys*, *Eomyops*) as arboreal, and species with four or less ridges (*Rhodanomys*, *Ritteneria*, *Pentabuneomys*, *Ligerimys*, *Estramomys*) as terrestrial. This ecomorphological distinction within eomyids is based on their dental pattern, which shows similarities to that of hamsters, for which it has been shown that pentalophodont species are forest-dwellers and tetralophodont species are open-country dwellers (Hershkovitz, 1997).

Invertivores are characterized by either pointed cusps in the dentition (mainly insectivorous diet) or round, flattened shapes (malacophagous diet). The latter category is not represented in the late Neogene data set. In this data set the invertivore category has a one-to-one correspondence to the order Lipotyphla. However, earlier time slices contain examples of rodents, for which an invertivorous diet can be inferred based on dental morphology (e.g. *Melissiodon*).

4.3. Direct comparison to the plant record

Recently, paleoprecipitation levels have been estimated for the early Late Miocene locality Rudabánya (Hungary) on the basis of both mammals and plants, allowing a direct comparison with the estimations based on both small and large mammals from this locality (Damuth et al., 2003). The small-mammal based mean MAP estimate based on Eq. (1) (Table 5) is 1235 mm/yr and falls within the range of 897–1297 mm/yr calculated on the basis of plants following the Coexistence Approach of Mosbrugger and Utescher (1997). A new approach based on large-mammal hypsodonty (Fortelius et al., 2002) also predicts a similar value (1190 mm/yr). The floral assemblage indicates a seasonality of precipitation of 86–89 mm/yr,

Table 6
Fossil localities and predicted precipitation levels

Locality	MN	Country	Selected up-to-date reference	MAP (mm)	MINP (mm)
La Grive St. Alban	7–8	France	de Bruijn et al. (1992)	1159	74
Steinheim (mittl.)	7–8	Germany	Heizmann and Reiff (2002)	672	25
Opole 2	7–8	Poland	Kowalski (1990)	1021	79
Castell de Barberà	7–8	Spain	Agustí (1990), Gibert (1975)	1178	62
Escobosa	7–8	Spain	López Martínez et al. (1977)	471	3
Hostalets de Pierola inf.	7–8	Spain	Agustí (1990), Gibert (1975)	729	14
Sant Quirze	7–8	Spain	Agustí (1990), Gibert (1975)	947	52
Toril	7–8	Spain	Daams et al. (1988), van den Hoek Ostende (pers. comm.)	550	42
Anwil	7–8	Switzerland	Engesser (1972)	1052	79
Bayraktepe 1	7–8	Turkey	Ünay (1981)	457	39
Yeni Eskihisar 1	7–8	Turkey	Sickenberg et al. (1975)	589	3
Götzendorf	9	Austria	Bachmayer and Wilson (1984), Rögl et al. (1993)	1189	83
Jujurieux	9	France	Mein (1999)	1086	54
Hammerschmiede	9	Germany	Fahlbusch and Mayr (1975)	830	64
Rudabánya	9	Hungary	Bernor et al. (2003)	1235	84
Belchatow A	9	Poland	Nadachowski (2001)	948	73
Can Llobateres 1	9	Spain	Agustí (1990), Gibert (1975)	1178	87
Can Ponsic 1	9	Spain	Agustí (1990), Gibert (1975)	947	52
Carrilanga	9	Spain	Daams et al. (1988), de Jong (1988)	622	19
Casas Altas	9	Spain	Besems and van de Weerd (1983), unpublished	655	36
Hostalets de Pierola sup.	9	Spain	Agustí (1990), Gibert (1975)	354	3
Masía de la Roma 3	9	Spain	van Dam et al. (2001)	504	19
Nombrevilla 1	9	Spain	Daams et al. (1988), unpublished	550	21
Pedregueras 2A	9	Spain	Daams et al. (1988), de Jong (1988)	618	29
Pedregueras 2C	9	Spain	Daams et al. (1988), unpublished	579	27
Peralejos 5	9	Spain	van Dam et al. (2001)	386	3
Nebelbergweg	9	Switzerland	Kälin and Engesser (2001)	963	54
Sinap Tepe 8A	9	Turkey	Lunkka et al. (1999), unpublished	435	3
Grytsev	9	Ukraine	Nesin and Nadachowski (2001)	1116	60
Kohfidisch	10	Austria	Bachmayer and Wilson (1980)	987	49
Suchomasty	10	Czech Rep.	Fejfar (1990)	1151	71
Ambérieu 2A	10	France	Mein (1999)	864	52
Ambérieu 2C	10	France	Mein (1999)	782	41
Douvre	10	France	Mein (1999)	1117	90
Lo Fournas 1993	10	France	Mein (1999)	860	48
Montredon	10	France	Aguilar (1982), Crochet and Green (1982)	912	28
Soblay	10	France	Mein (1999)	1074	69
Kalfa and Buzhor	10	Moldavia	Nesin and Nadachowski (2001)	514	3
Can Casablanques 2	10	Spain	Agustí (1990)	471	3
La Roma 1	10	Spain	van Dam et al. (2001)	566	3
La Roma 2	10	Spain	van Dam et al. (2001)	314	3
Masía de la Roma 11	10	Spain	van Dam et al. (2001)	574	18
Masía de la Roma 4C	10	Spain	van Dam et al. (2001)	354	3
Masía de la Roma 7	10	Spain	van Dam et al. (2001)	622	19
Masía de la Roma 9	10	Spain	van Dam et al. (2001)	756	27
Masía del Barbo 2A	10	Spain	van Dam et al. (2001)	740	19
Masía del Barbo 2B	10	Spain	van Dam et al. (2001)	592	16
Peralejos 4	10	Spain	van Dam et al. (2001)	550	21
Peralejos C	10	Spain	van Dam et al. (2001)	471	3
Puente Minero 2	10	Spain	van Dam et al. (2001)	464	22
Terrassa	10	Spain	Agustí et al. (1984)	711	21
Bayraktepe 2	10	Turkey	Ünay (1981)	530	3
Karaözü	10	Turkey	Sümengen et al. (1989)	403	16
Eichkogl	11	Austria	Daxner-Höck (1980), Rabeder (1970)	976	56
Ambérieu 1	11	France	Mein (1999)	783	54

(continued on next page)

Table 6 (*continued*)

Locality	MN	Country	Selected up-to-date reference	MAP (mm)	MINP (mm)
Ambérieu 3	11	France	Mein (1999)	834	50
Bernardière	11	France	Mein (1999)	643	3
Dionay	11	France	Mein (1999)	739	32
Lobrieu	11	France	Mein (1999)	729	31
Mollon	11	France	Mein (1999)	524	29
Dorn Dürkheim	11	Germany	Franzen and Storch (1999)	971	59
Lefkon	11	Greece	de Bruijn (1989)	662	31
Csákvár	11	Hungary	Kretzoi (1951), Mészáros (1996)	424	3
Sümeg	11	Hungary	Kretzoi (1984), Mészáros (1996)	913	21
Crevillente 2	11	Spain	Montoya (1994)	504	19
La Gloria 10	11	Spain	van Dam et al. (2001)	386	3
Los Aguanaces 1	11	Spain	van Dam et al. (2001)	404	3
Los Aguanaces 3	11	Spain	van Dam et al. (2001)	354	3
Masada Ruea 2	11	Spain	van Dam et al. (2001)	435	3
Peralejos D	11	Spain	van Dam et al. (2001)	314	3
Puente Minero 3	11	Spain	van Dam et al. (2001)	471	3
Tortajada A	11	Spain	van Dam et al. (2001)	326	3
Vivero de Pinos	11	Spain	van Dam et al. (2001)	471	3
Hayranlý 1	11	Turkey	Unpublished	616	13
Novoelizavetovka 2	11	Ukraine	Nesin and Nadachowski (2001)	378	15
Mont Lubéron	12	France	Mein (1999)	504	19
Pikermi 4	12	Greece	de Bruijn (1976)	605	22
Tardosbánya	12	Hungary	Kordos (1987), Mészáros (1998), Kordos (pers. comm.)	1057	72
Concud 2	12	Spain	van Dam et al. (2001)	544	3
Concud 3	12	Spain	van Dam et al. (2001)	688	14
Concud Barranco	12	Spain	van Dam et al. (2001)	566	3
Crevillente 15	12	Spain	Montoya (1994)	432	17
Cubla	12	Spain	van Dam et al. (2001)	628	3
Los Mansuetos	12	Spain	van Dam et al. (2001)	544	3
Masada del Valle 2	12	Spain	van Dam et al. (2001)	442	3
Masada del Valle 3	12	Spain	van Dam et al. (2001)	530	3
Masada del Valle 4	12	Spain	van Dam et al. (2001)	471	3
Masada del Valle 5	12	Spain	van Dam et al. (2001)	471	3
Masada Ruea 3	12	Spain	van Dam et al. (2001)	386	3
Masada Ruea 4	12	Spain	van Dam et al. (2001)	424	3
Tortajada	12	Spain	van Dam et al. (2001)	566	3
Tortajada C	12	Spain	van Dam et al. (2001)	628	3
Tortajada D	12	Spain	van Dam et al. (2001)	566	3
Villalba Baja 2	12	Spain	van Dam et al. (2001)	566	3
Düzyayla	12	Turkey	de Bruijn et al. (1999)	644	42
Novoukrainka 2 (unit)	12	Ukraine	Nesin and Nadachowski (2001)	486	21
Lissieu	13	France	Mein (1999)	768	47
Ano Metochi 3	13	Greece	de Bruijn (1976)	202	3
Maramena	13	Greece	Schmidt-Kittler et al. (1995)	818	47
Polgárdi (=Polgárdi 2)	13	Hungary	Freudenthal and Kordos (1989), Mészáros (1999)	589	3
Baccinello V3	13	Italy	Hürzeler and Engesser (1976), Engesser (1989)	358	25
Brisighella	13	Italy	de Giuli (1989)	491	27
Alcoy barranco	13	Spain	Montoya (1997)	386	19
Arquillo 4	13	Spain	Mein et al. (1990)	435	3
Bacochas 1	13	Spain	Sesé (1989)	236	3
Celadas 2	13	Spain	Adrover et al. (1993)	544	3
La Gloria 5	13	Spain	Adrover et al. (1993)	377	3
La Gloria 6	13	Spain	Mein et al. (1990)	498	16
Las Casiones	13	Spain	van Dam et al. (2001)	530	3
Las Casiones superior	13	Spain	van Dam et al. (2001)	544	3
Masada del Valle 7	13	Spain	van Dam et al. (2001)	566	3

Table 6 (*continued*)

Locality	MN	Country	Selected up-to-date reference	MAP (mm)	MINP (mm)
Valdecebro 3	13	Spain	van Dam et al. (2001)	606	3
Valdecebro 6	13	Spain	Adrover et al. (1993)	435	3
Amasya	13	Turkey	Sickenberg et al. (1975), Engesser (1980), Ünay and de Bruijn (pers. comm.)	404	3
Kavurca	13	Turkey	Sickenberg et al. (1975), Engesser (1980), Ünay and de Bruijn (pers. comm.)	467	13
Odessa	13	Ukraine	Nesin and Nadachowski (2001)	460	31
Montpellier	14	France	Michaux (1969)	830	64
Vendargues	14	France	Barrière and Michaux (1968), Crochet (1986)	504	19
Maritsa 1	14	Greece	van der Meulen and van Kolfschoten (1986)	170	13
Novaya Andriashevka	14	Moldavia	Pevzner et al. (1996)	480	25
Podlesice	14	Poland	Kowalski (1990)	1012	42
Dranic 0	14	Romania	Radulescu et al. (2000)	785	3
Antipovka	14	Russia	Pevzner et al. (1996)	386	3
Chugunovka	14	Russia	Pevzner et al. (1996)	386	19
Grebeniki 2	14	Russia	Pevzner et al. (1996)	290	15
Obukhovka 1	14	Russia	Pevzner et al. (1996)	236	3
Celadas 14	14	Spain	Mein (pers. comm.)	354	3
Celadas 8	14	Spain	Mein (pers. comm.)	471	3
Celadas 9	14	Spain	Adrover et al. (1993)	354	3
La Gloria 4	14	Spain	Adrover et al. (1993)	367	3
La Juderia	14	Spain	Mein (pers. comm.)	354	3
Lomas de Casares 2	14	Spain	Mein (pers. comm.)	236	3
Lomas de Casares 5	14	Spain	Mein (pers. comm.)	606	3
Orrios 1	14	Spain	van de Weerd (1976), Mein (pers. comm.)	283	3
Peralejos E	14	Spain	Adrover et al. (1993)	372	3
Purcal 4	14	Spain	Martín-Suárez et al. (1998)	387	33
Villalba Alta Rio 1	14	Spain	Mein (pers. comm.)	303	3
Dinar–Akçaköy	14	Turkey	Sickenberg et al. (1975), Engesser (1980), Ünay and de Bruijn (pers. comm.)	357	18
Mont Hélène	15	France	Aguilar et al. (1986), Crochet (1986)	414	23
Perpignan	15	France	Aguilar and Michaux (1984)	344	27
Séte	15	France	Aguilar and Michaux (1984)	83	3
Wölfersheim	15	Germany	Dahlmann (2001)	994	49
Csarnota 2	15	Hungary	Jánossy (1986)	820	47
Ewa Cave 3	15	Poland	Nadachowski (1990)	745	37
Weze 1	15	Poland	Kowalski (1990)	878	33
Dranic 1	15	Romania	Radulescu et al. (2000)	471	3
Dranic 2	15	Romania	Radulescu et al. (2000)	358	25
Dranic 3	15	Romania	Radulescu et al. (2000)	471	3
Ivanovce	15	Slovakia	Fejfar (1990)	501	31
El Arquillo 3	15	Spain	Mein and Adrover (1977)	515	12
Escorihuela B	15	Spain	van de Weerd (1976), Mein (pers. comm.)	356	14
Escorihuela D	15	Spain	Mein (pers. comm.)	314	3
La Calera	15	Spain	Pérez and Soria (1990)	265	3
La Gloria 2	15	Spain	Mein (pers. comm.)	273	14
La Gloria 3	15	Spain	Mein (pers. comm.)	393	13
Layna	15	Spain	Pérez and Soria (1990)	258	14
Lomas de Casares 1	15	Spain	Mein et al. (1990)	283	3
Orrios 3	15	Spain	Mein (pers. comm.)	356	14
Orrios 7	15	Spain	Mein et al. (1990)	202	3
Orrios 9c	15	Spain	Mein (pers. comm.)	354	3
Poblado Iberico	15	Spain	Mein (pers. comm.)	303	3
Sarrión 2	15	Spain	Adrover (1986), Mein (pers. comm.)	336	14
Villalba Alta 1	15	Spain	Mein et al. (1990)	212	3
Villalba Alta 3	15	Spain	Mein (pers. comm.)	300	3
Villalba Alta 4	15	Spain	Mein (pers. comm.)	533	17
Villalba Alta Rio 2	15	Spain	Mein (pers. comm.)	318	13

(continued on next page)

Table 6 (*continued*)

Locality	MN	Country	Selected up-to-date reference	MAP (mm)	MINP (mm)
Villalba Alta Rio 2A	15	Spain	Mein (pers. comm.)	142	3
Vue des Alpes	15	Switzerland	Bolliger et al. (1993)	961	26
Çalta	15	Turkey	Sen et al. (1998)	386	19
Odessa Catacombs	15	Ukraine	Pevzner et al. (1996)	83	3
Balaruc 2	16	France	Bachelet (1990), Crochet (1986)	643	21
Seynes	16	France	Bachelet (1990), Crochet (1986)	466	15
Gundersheim 1	16	Germany	Dahlmann (2001)	712	29
Hambach 11	16	Germany	Mörs et al. (1998)	1208	77
Rebielice Królewskie 1	16	Poland	Kowalski (1990)	885	39
Podari	16	Romania	Radulescu et al. (2000)	820	15
Cherevichnoe 2 (unit)	16	Russia	Nesin and Nadachowski (2001)	262	16
Obukhovka 2 (unit)	16	Russia	Nesin and Nadachowski (2001)	326	3
Hajnácka 1	16	Slovakia	Sabol (2001)	711	21
Concud Estación 1	16	Spain	Mein (pers. comm.)	283	3
Concud Estación 2	16	Spain	Mein et al. (1990)	471	3
Escorihuela	16	Spain	van de Weerd (1976), Mein (pers. comm.)	530	3
Moreda	16	Spain	Ruis Bustos (2002)	358	25
Sarrión 1	16	Spain	Adrover (1986), Mein (pers. comm.)	273	14

which is a moderate amount. A much more homogeneous rainfall distribution is predicted by the small mammals, with an estimate of 84 mm (confidence interval ± 20 mm) in the driest month.

Direct plant–small mammal comparison is also possible between the small-mammal fauna of Götzendorf and the nearby and time-equivalent floras of Vösendorf and Laaerberg (Austria, Bruch et al., 2006-this volume). The small-mammal based MAP estimate of 1189 mm/yr is close to the plant-based estimates of 1036–1096, and 897–1187 mm, respectively. A third opportunity for comparison is offered by the time-equivalent fauna and flora from the Pliocene Reuverian clays (local Zone 11) of the Lower Rhine Basin (NE Germany). The mean estimate for the small-mammal fauna Hambach Mine (1208 mm) fits reasonably well to the macroflora-based estimate for the neighboring Fortuna Garsdorf Mine (979–1076 mm) (Utescher et al., 2000). The Miocene–Pliocene boundary interval in southern Spain allows a comparison at the dry side of the spectrum: the small-mammal based estimate of 387 mm (Purcal 4) is very close to the values around 400 mm estimated on the basis of pollen (Fauquette et al., 1999). In some areas discrepancies can be noted: e.g. MN14-correlative faunas from southwest France (Montpellier, Vendargues), however, show lower values (830 and 504 mm, respectively) than pollen (mean values of 1200–1350 mm). Nevertheless, there is a high overall degree of consistency between the independent estimates based on flora and fauna, and there seems presently to be no reason for an additional calibration of the small-mammal based estimates.

4.4. Precipitation maps and curves

Eqs. (1) and (3) (Table 5) were applied to a data set of 191 more or less complete late Neogene European faunas (Table 6). Part of the data is stored in the Neogene Old World (NOW) database (http://www.helsinki.fi/science/now). Plots of arboreality against invertivory (Fig. 8a–b) show the positions of the recent localities (Table 1) within the cloud of fossil localities. Evidently, many fossil localities show much higher values of arboreality and invertivory than the recent localities, suggesting that more densely forested and wetter environments than today have existed during the late Neogene. Fig. 8c shows a plot of estimated MINP against MMP (= MAP/12). It should be noted that (even given the broad confidence intervals) there is no inconsistency in the predictions in the sense that points plot above the dashed line (the line of no seasonality, i.e. minimum and mean precipitation values are equal). The scatter plot covers a wide variety in precipitation regimes, including very equable ones (close to the line), without recent analogues. There is no indication for regimes that are more seasonal than today's Mediterranean ones.

Maps are constructed for European Mammal Neogene (MN) Units 7/8 to 16 (Figs. 9 and 10) with the program MAP INFO, using an inverse-distance weighting algorithm (see figure captions for program options). Trends and gradients have to be interpreted carefully because data coverage changes from time to time and region to region. Color-coding in Fig. 9 is consistent with that used by Fortelius et al. (2002, 2006-this

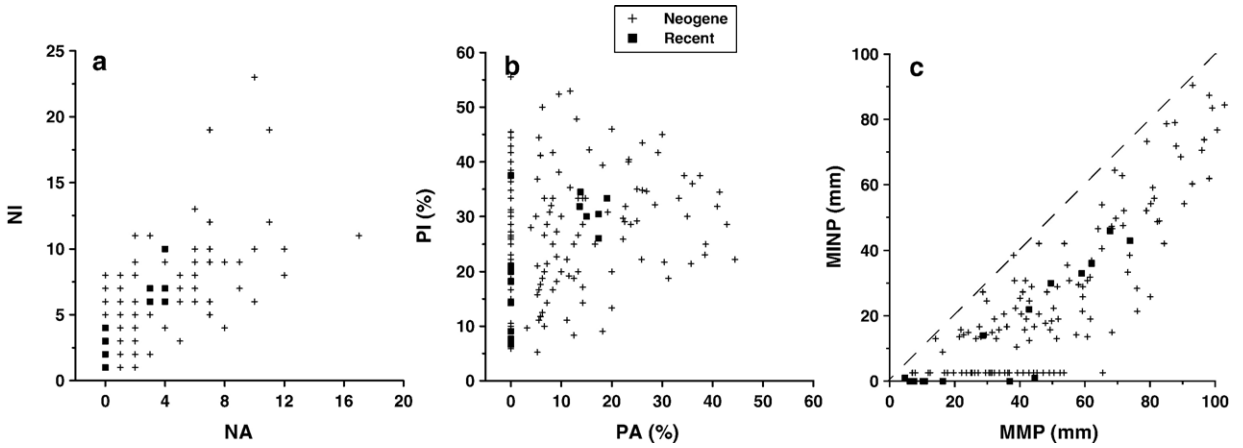

Fig. 8. Scatter plots including both Recent (Table 1) and late Neogene (Table 6) localities. (a) Invertivory Richness against Arboreality Richness, (b) Invertivory Index against Arboreality Index, (c) MINP against MMP (= MAP/12).

volume). The transition from white to gray values in Fig. 10 more or less corresponds to the transition from open woodland–scrubland to closed forest as observed in southern Europe today, which occurs at a value of about 20 mm in the driest month. Maps of recent MAP and MINP (Figs. 9j and 10j) are based on data from Müller (1996) and KNMI (1998) and are smoothed using the same values for the spatial interpolation parameters (caption Fig. 9). Curves per region (MN unit scale) are shown in Figs. 11 and 12, and Fig. 13 shows a more detailed curve is shown for the dense record of central Spain.

5. Results and comparison to other terrestrial proxies

5.1. The basic geographic gradients

The mean annual precipitation maps (Fig. 9) clearly show the presence of an extensive wet zone in NW and central Europe during almost all intervals. I will refer to this zone as the European Temperate Wet Zone (ETWZ), loosely defined as an area with rainfall levels between 800 and 1200 mm/yr, corresponding to the blue colors in Fig. 9. The maps suggest that the area of the ETWZ was wetter than today during most of the late Neogene (Fig. 9j). The Mediterranean and eastern Europe were probably drier than today, particularly after 7–6 Ma, resulting in sharp north–south and east–west gradients. Also the minimum monthly precipitation maps (Fig. 10) show sharp gradients, especially at 10–9 Ma. It should be noted that precipitation zones were probably more zonal in southern Europe than shown on the maps. This is due to the lack of mainland data for Italy, a large part of which consisted of islands until ~7 Ma. Because the spatial interpolation method uses a search radius, the ETWZ is projected far into present-day Italy. A more zonal pattern emerges at MN13, for which Italian data are available (Figs. 9f and 10f).

Strong north–south gradients in Late Miocene humidity were also found in a previous study using rodent relative abundances (van Dam and Weltje, 1999). A similar trend is indicated by large-mammal faunas, which differ strongly between central and southern Europe, with forest or dense woodland communities in the north and open-country "Pikermian megafaunas" in the south and southeast during the Late Miocene (Bernor, 1984). Also large-mammal hypsodonty (Fortelius et al., 2002, 2006-this volume) shows the existence of both east–west and north–south gradients.

The presence of sharp precipitation gradients on the European continent during the late Neogene is consistent with results from paleobotanical/palynological studies. On the basis of a coastal series of on- and offshore pollen records, Fauquette et al. (1999) infer a mean annual precipitation gradient for the basal Pliocene (5.3–5 Ma), which starts in northernmost Africa and southernmost Spain (mean value 400–450 mm/yr), runs through S Catalonia (670 mm), shows a sharp rise in N Catalonia (1200 mm), and ends in S France (1300–1350 mm). These results agree very well with the small-mammal based results at 5 Ma (Fig. 9g), with similar absolute values for Spain and the same sharp increase at the level of Catalonia. Vegetation-type reconstructions show that this increase represents the transition from xerophytic woodland/scrubland to warm mixed forest and broad- or needle-leaved evergreen forest (Fauquette et al., 1999). The early Pliocene precipitation gradient extends further northward into the "West European domain", characterized by *Taxodium*

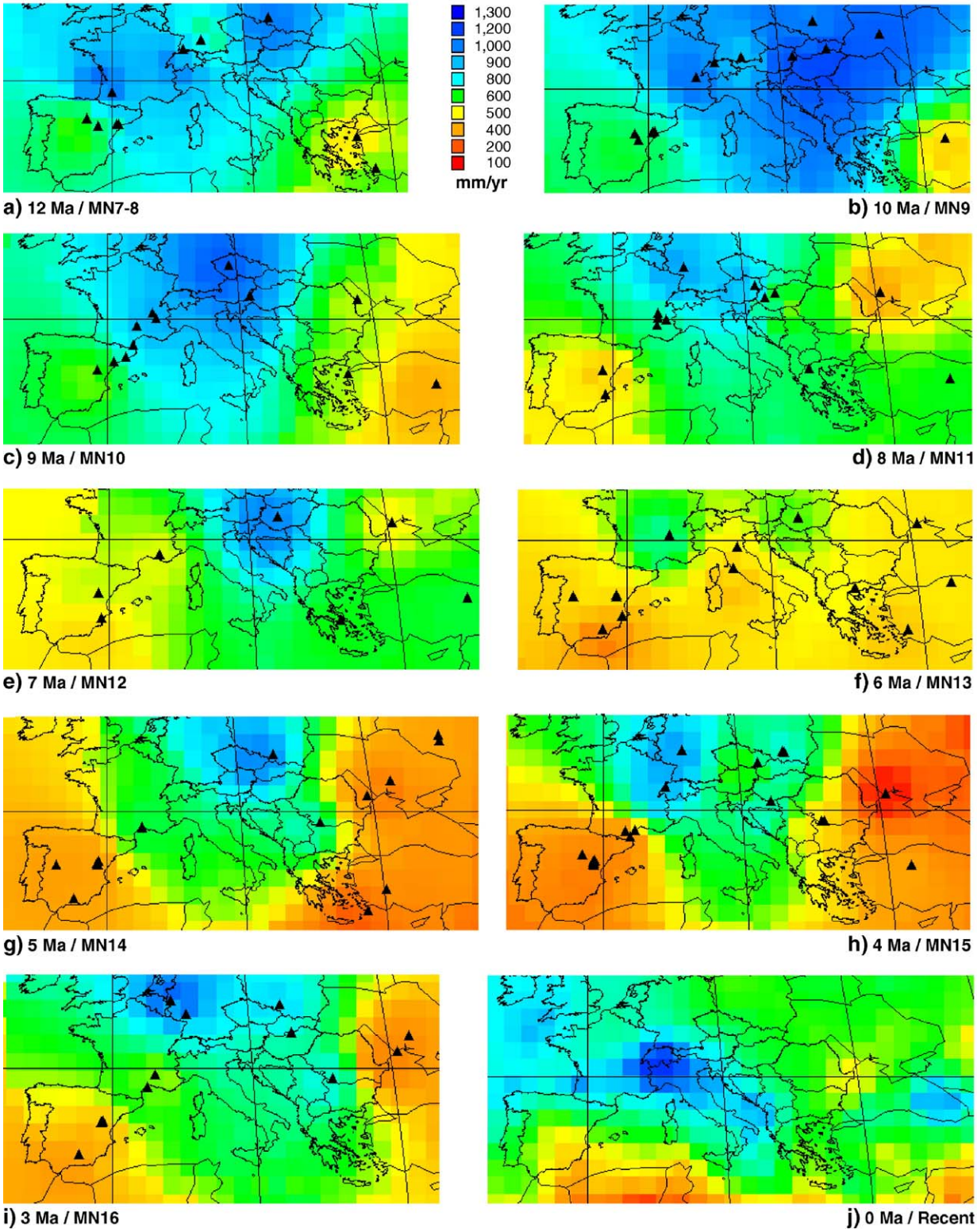

Fig. 9. Mean annual precipitation (MAP) maps per time slice (numerical ages and corresponding MN units). Spatial interpolation consists of an inverse-distance weighted algorithm (program MAPInfo Professional 6.0) with the following settings: distance exponent 2, cell size 100 km, search radius 1000 km, grid border 200 km. Input for maps a–i: values in Table 6. Input for map j: values from 192 meteorological stations (Müller, 1996; KNMI, 1997).

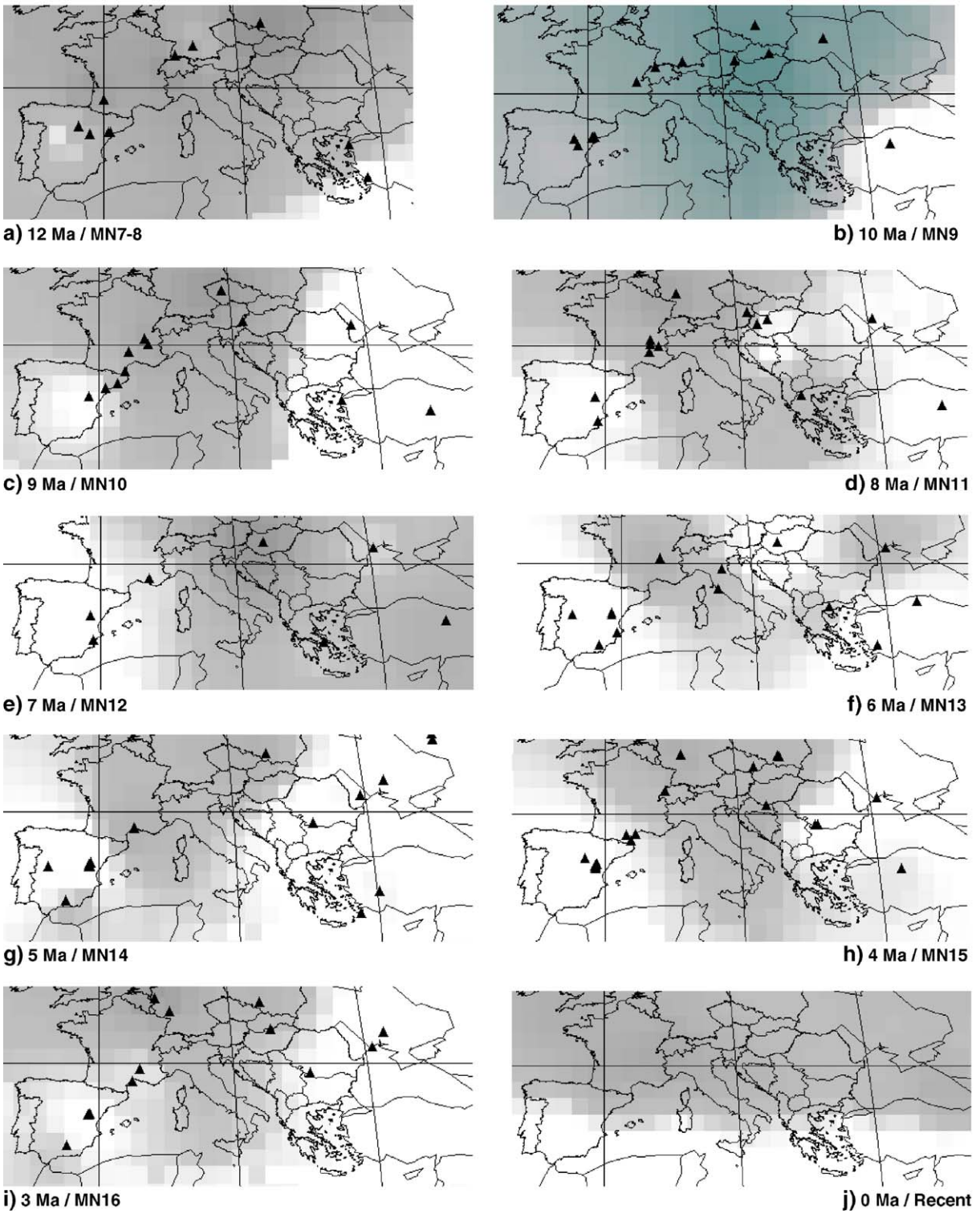

Fig. 10. Precipitation in the driest month (MINP) per time slice (numerical age/MN Unit). Spatial interpolation and data sources: see caption of Fig. 9. In order to optimally contrast open with closed landscapes, gray-value inflection points were set at 0 mm (white), 15 mm (white), 25 mm (light gray) and 100 mm (dark gray). 20 mm is more or less the boundary between forest and woodland–scrubland in S Europe as observed today.

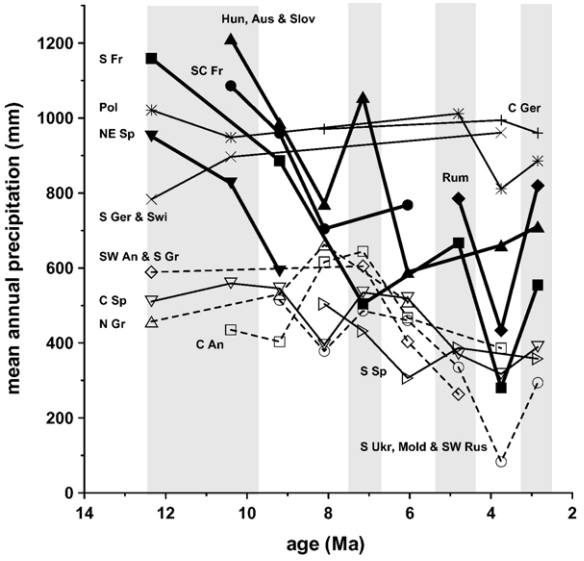

Fig. 11. Mean annual precipitation (MAP) trends per region. Localities are grouped into 14 regions: central Spain, southern Spain, northeastern Spain, southern France, south–central France, southern Germany and Switzerland, central Germany, Poland, Hungary–Austria–Slovakia, Rumania, Southern Ukraine–Moldavia–southwestern Russia, southwestern Anatolia–southern Greece, northern Greece. Gray bars indicate periods of increased rainfall.

swamps at low altitudes and deciduous vegetation at mid-altitudes (Suc et al., 1999). Unfortunately, the late Neogene flora from interior parts of Spain is poorly known. A ~11 Ma old sequence from the Duero Basin (Spain) has yielded a set of floras including a significant proportion of Poaceae, Chenopodiaceae and Amaranthaceae, indicating the presence of a woodland/steppe environment (Rivas-Carballo, 1991).

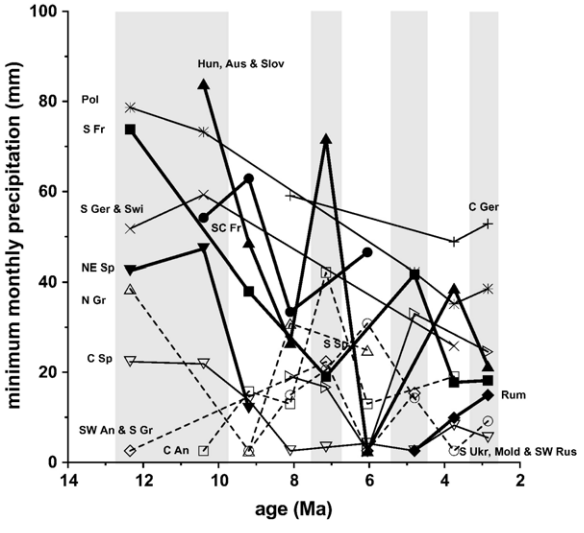

Fig. 12. Minimum monthly precipitation (MINP) trends per region. For regions: see caption of Fig. 11. Gray bars indicate periods of increased rainfall.

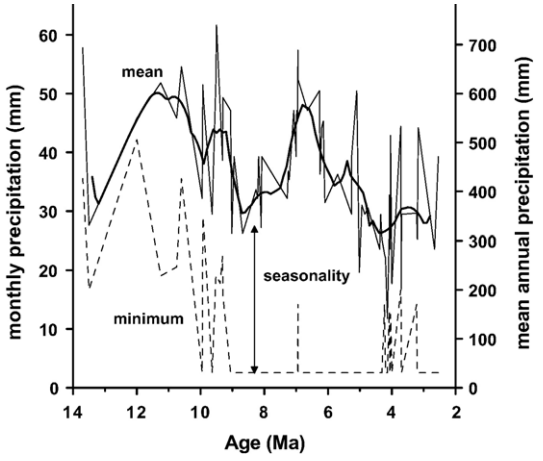

Fig. 13. Mean (MAP, MMP) and minimum monthly precipitation (MINP) trends for central Spain (Teruel and Calatayud–Daroca Basins). The bold line represents a seven-point moving average of interpolated (100 kyr equal-spacing) MAP values. A measure of seasonality (SEASL) is calculated as MAP/12 − MINP = MMP − MINP. Ages of the Middle Miocene localities Armantes 7 (local Zone F) and Toril after Daams et al. (1999). Ages of the Late Miocene localities after van Dam (1997), van Dam et al. (2001), Alcalá et al. (2000), Abdul Aziz et al. (2004), and Abdul Aziz (pers. comm.). Ages of Pliocene localities after Opdyke et al. (1997) and Agustí et al. (2001) with biostratigraphic and biochronological interpolations after Mein et al. (1990).

Bruch et al. (2006-this volume) also found a distinct precipitation gradient in the eastern part of Europe between early Tortonian (11–9 Ma) floras from central Europe (including Bulgaria) with mean levels between 1000 and 1300 mm/yr, and a flora from S Greece (Crete) with an estimated mean level of 750 mm/yr. The presence of a sharp gradient to the east, visible in most of the small-mammal based plots, is consistent with pollen data from the Black Sea area (mainly Ukraine), which indicate an open, steppe-type of environment, sometimes with forest patches (forest–steppe), throughout most of the late Neogene (Jones and Simmons, 1997; Svelitskaya, 1999).

The present-day peak position of the ETWZ (Switzerland, SE France and NW Italy) is situated in a more southern position when compared to the Neogene situation, and associated with orographic effects from the Alps. Unfortunately, the elevation history of the Alpine region is not well known. Pollen indicates ~1000 m of Plio–Pleistocene uplift in the southern Alps (Pérez Vila et al., 2001). The high small-mammal based rainfall estimate of 950–1000 mm level at the Swiss locality Vue des Alpes (Fig. 9h) could indicate a reasonably high topography by 4 Ma. On the other hand,

smooth Mediterranean to central European gradients in plant communities are known to have existed into the Plio– or even Pleistocene, indicating a generally low relief (1500 m?) until then (van der Burgh, pers. comm.). Pollen records from the Pyrenees indicate that elevation could have increased in that region between 6.5 and 5.3 Ma (Pérez Vila et al., 2001). Such uplift could explain the increase of the precipitation contrasts between France and Spain during the Pliocene (Fig. 9).

5.2. The Late Miocene: contraction/shifting of the European Temperate Wet Zone (ETWZ)

After relatively dry Middle Miocene conditions between 16 and 13 Ma (van der Meulen and Daams, 1992; unpublished small-mammal based precipitation predictions), precipitation levels increase at 13–11 Ma (latest Middle Miocene, MN7–8-correlative) (Figs.9a and 10a) and culminate between 11 and 10 Ma, i.e. in the earliest Late Miocene (earliest Tortonian, MN9-correlative). MAP reaches levels between 1100 and 1250 mm/yr in a large area from NE Spain to the Ukraine. Also MINP levels are exceptionally high during this interval (over 60 mm in the driest month in central Europe), suggesting the presence of a seasonally very homogeneous rainfall regime. The MAP levels in central Spain are much lower, around 600 mm/yr, but they are still high compared to other time slices. Central Anatolia is the only dry region during this time.

Between 10 and 5 Ma the southern boundary of the ETWZ is migrating slowly towards the north and northwest, to reach its most northern position (north of the map area in Fig. 9f) during Messinian times (7–5 Ma, MN13-correlative). During the Messinian annual rainfall is 600 mm in central Europe (Hungary) and 300–500 mm in Spain. Curves per region (Figs. 11 and 12) clearly show the main trend of contraction and/or northward shifting and show that changes were largely confined to the intermediate latitudes (43–50°) of central Europe, i.e. France and Hungary–Austria–Slovakia. Although data are lacking for some intervals, there is no evidence of substantial change in MAP in the more northern areas (Poland, Germany–Switzerland), where levels remain at 800–1000 mm/yr. Similarly, southern Mediterranean rainfall mostly remains within the 400–600 mm range during the Late Miocene.

Contraction of a central European humid zone has also been inferred on the basis of large mammals from the early Late Miocene. E.g., the fauna from Dorn–Dürkheim in Germany (~ 8 Ma) contains forest-adapted forms that originated in southwestern, southeastern and eastern Europe (Franzen and Storch, 1999). These observations are consistent with the recognition of the Lower Rhine Basin as a refuge area for broad-leaved evergreen flora elements (van der Burgh, 1987).

The observed shrinking (or northward shift) of the ETWZ (Fig. 9) between 8 and 6–5 Ma fits results from paleobotanical and palynological studies. No major change in pollen floras is noted in Sicily, N Italy and SE France during this time (Suc and Bessais, 1990; Suc et al., 1999). Similarly, precipitation reconstructions for the north, e.g. Germany (Utescher et al., 2000) and floras from the Central Paratethys (Bernor et al., 1988) do not indicate a major change in rainfall during the Late Miocene. However, in agreement with the small-mammal results, aridification trends have been observed at intermediate latitudes, e.g. Bulgaria around 11 Ma (Ivanov et al., 2002) and France (Rhone Valley) around 9 Ma (Farjanel and Mein, 1984). Central Anatolia remains outside the ETWZ during the studied interval. The unexpected rise in precipitation in this area at 8–7 Ma will be discussed below.

5.3. The early–middle Late Miocene (10–8 Ma): establishment of a dry season

The decrease in MINP in western and central Europe is stronger and occurs earlier (10–8 Ma) than the decrease in MAP (Figs. 11 and 12), suggesting that the establishment of a dry season was the first step in the aridification process. (Rainfall during the wettest months may even have increased in northern central Europe, as suggested by the decreasing MINP level and more or less constant MAP level in Poland and Germany–Switzerland.) More specifically, MINP levels in France and Hungary–Austria–Slovakia reach 15–25 mm by 9–8 Ma, which is within the present-day Mediterranean range of values. In central Spain mean levels go down from 20–25 to 0 mm. This “opening up” of Spain between 10 and 8 Ma is illustrated in Fig. 10b–d. Fig. 13 indicates that the establishment of a truly dry season (MINP close to 0) in central Spain occurred around 8.5 Ma.

Large-mammal studies support the small-mammal based results. An important aridification around 9 Ma in the Mediterranean region itself has been inferred on the basis of ruminants (Köhler, 1993). Furthermore, the interval of 10–8 Ma exactly corresponds to the time that many forest-adapted large mammals migrate to central Europe, which functioned as a refuge area for these groups (Franzen and Storch, 1999; see above). By contrast, hominoids move southward to disappear finally from the Mediterranean rim around 9–8 Ma

(see Fortelius and Hokkanen, 2001). Southward migration suggests a low tolerance for reduced (winter) temperatures, which seems to be related to their preference for evergreen vegetation and associated whole-year availability of fruits (see Suc et al., 1999). Apparently, the Mediterranean temperature regime between 12 and 10 Ma was not harsh enough to force hominoids to leave the area, leaving the establishment of a dry season after 10 Ma as the most probable reason for their European extinction.

There is no compelling reason to believe that seasonal drying did not occur during summer, as it does today. The absence of C4 vegetation in the eastern Mediterranean suggests that summers were at least not wet there (Quade et al., 1994).

5.4. Temporary increase in precipitation (8–7 Ma)

A short return to more humid conditions at 8–7 Ma seems to have occurred in various areas. The predictions suggest a precipitation increase during the dry season (most probably summer) precipitation for Anatolia, Greece, Hungary (high values in Fig. 12, see the map of Fig. 10e). The curves for central Spain suggest that the increase did not occur during the dry season, and an increase of winter precipitation can be hypothesized for this region (almost no MINP increase, Fig. 13). Large-herbivore mean-hypsodonty maps also show generally more humid conditions at MN12 than at MN11 and MN13 (Fortelius et al., 2006-this volume). The observation that the "Pikermian woodland biome" (Solounias et al., 1999), which supported a rich open-country large-mammal fauna, reached its maximum extension during MN12-correlative times (Fortelius et al., 1996) is consistent with the prediction of a temporary amelioration of conditions.

5.5. The early Pliocene (5–4 Ma): stronger gradients and decrease in winter precipitation

The Pliocene maps show sharp east–west rainfall contrasts. While MAP levels remain at late Miocene levels in northern–central Europe, there is continuous aridification in the east. Eastern aridity peaks around 4 Ma (later Zanclean, MN15-correlative) in Anatolia, the Black Sea region, Rumania, and perhaps also Poland. Since MINP is already low, it can be hypothesized that the aridification is largely due to the lowering of winter precipitation. A drop in winter precipitation can also be inferred for central Spain (Fig. 13). The curve shows a conspicuous minimum in MAP around 4 Ma, whereas MINP shows an increase at the same time, suggesting a dry, but seasonally homogeneous regime.

An overall decrease in winter precipitation fits very well the precipitation reconstructions based on floras from the Lower Rhine Embayment of Utescher et al. (2000), who also note a major decrease in precipitation in the wettest month between 5 and 4 Ma. Also with regard to increasing north–west and east–west contrasts the floral record provides confirming evidence. Firstly, Pliocene floral assemblages north and south of the Pyrenees–Alps–Carpathian line show increased provinciality compared to the Miocene (Mai, 1995). Secondly, large tracts of deciduous hardwood forests, which were present in southwestern Asia and southeastern Europe until the Late Miocene, had probably disappeared by the Pliocene (Singh, 1988). By contrast, relatively humid conditions remained in W Georgia, which functioned as a refuge area for plants (Shatilova and Ramishvili, 1984) because of the nearby presence of the Eastern Paratethys Sea. In Spain, the ongoing aridification results in a sharpening of the western European precipitation gradient, a phenomenon that also has been observed on the basis of pollen (Fauquette et al., 1999; see above). Large-mammal mean hypsodonty results confirm these patterns, indicating increasing precipitation in western Europe and increasing aridity in the eastern Mediterranean and Asia (Fortelius et al., 2006-this volume).

5.6. Middle Pliocene (3 Ma): precipitation increase in the east

The maps for 3 Ma (3.3–2.5 Ma, MN16-correlative, lower Piacenzian) have to be interpreted with care, because strong wet–dry cycles related to the Plio–Pleistocene Northern Hemisphere glaciations start to develop from 2.8 Ma onwards (Fauquette et al., 1998). Nevertheless, it is remarkable that an increase in precipitation can be observed in the same regions where a minimum was reached around 4 Ma (Fig. 9). Again, the rise is especially in MAP, suggesting a recovery of winter precipitation to the levels of 5 Ma.

It is tempting to correlate this precipitation increase to the "mid-Pliocene optimum", a globally recognized interval of increased temperatures around 3 Ma, just preceding the intensification of the N Hemisphere glaciations (Crowley, 1996). This interval is characterized by a sharp rise in winter temperatures, particularly at high latitudes. A change towards wetter conditions and increased continent-inward transport of moisture (Thompson and Fleming, 1996) has been inferred for the mid-latitudes. It should be noted, however, that the mid-Pliocene optimum is only faintly (if at all)

recognizable in western Mediterranean pollen records (Suc et al., 1995; Fauquette et al., 1999).

6. Discussion: explaining European late Neogene precipitation trends

6.1. Regional tectonic and geographic control

Late Neogene changes in the paleogeography and paleotopography of Europe are mainly related to African–Eurasian collision. These changes include the uplift of mountain ranges such as Alps, Pyrenees, Carpathians and Caucasus and the shrinking of the Paratethys Sea. The general consensus is that high topographies were not attained before Plio–Pleistocene times, implying that uplift might at least be held partly responsible for the ongoing aridification of parts of eastern Europe and Spain during the Pliocene. The shrinking of the Eastern Paratethys during the Pliocene to what are now the Caspian and Black Sea might additionally have explained aridification in that area.

On the other hand, the opening of the Aegean seaway between the Mediterranean and Black Sea and the expansion of the Eastern Paratethys during transgression might have led to the temporary precipitation increase in Anatolia around 8–7 Ma (Figs. 9d–e and 10e) because of the increased advection of atmospheric moisture. Generally, the proximity and off-wind position with regard to relatively warm seawater will have resulted in local centers of higher precipitation. Such areas commonly function as refuges for (partly evergreen) vegetation and associated fauna. Examples are western Georgia (Eastern Paratethys), and parts of Italy and the Balkan peninsula (Mediterranean), and also northwestern Germany (North Sea).

6.2. Global temperature trends and shifting subtropical high pressure zone

Whereas periods of major cooling (glacial intervals) are expected to be drier globally, there is ample evidence for cooling of Europe and NE Atlantic between 12 and 10–9 Ma, the interval during which the ETWZ shows a major southward extension. This negative correlation between humidity and temperature for the western part of Europe was inferred previously (van Dam and Weltje, 1999). General cooling between 12 and 10–9 Ma is evidenced by the replacement of tropical by deciduous vegetation in both central Europe and the northern Mediterranean area. In addition, warm-adapted *Avicennia* mangroves disappear from the latter area (Suc et al., 1999; Kovar-Eder, 2003). This cooling event is correlated by Suc et al. (1999) to the first of their two major Neogene breaks observed in the more or less continuous pollen records of N Italy and SW France (the second break corresponding to the development of the latest Pliocene *Artemisia* steppes, linked to the onset of the Northern Hemisphere glaciations). More evidence for cooling comes from Iceland, where a floral shift points to a major cooling of 10 °C between 10 and 9.5 Ma (Mudie and Helgason, 1983). Climate predictions based on floras from Germany and Bulgaria point to a decrease of ~3 and ~2 °C in winter temperatures, respectively, around this time (Utescher et al., 2000; Ivanov et al., 2002). Marine evidence for cooling consists of ice-rafted debris in the polar Atlantic at 10–9 Ma, indicating incipient N Hemisphere glaciations (Thiede et al., 1998). In the Mediterranean, an increase of cool-water planktonic foraminifer species is noted between 12.1 and 9.8 Ma with an additional peak of cool-water neogloboquadrinids around 9 Ma (Turco et al., 2001). Although global deep-sea oxygen isotope do not show a significant break or excursion around this time, 10 Ma is about the time the oxygen isotope ratios reach again the high values which were attained during the Early Oligocene glaciation (Zachos et al., 2001). This suggests that some critical climatic threshold may have been surpassed by early Late Miocene times.

The penetration of large amounts of moisture deep into eastern Europe between 12 and 10 Ma (e.g. Fig. 9) suggests the presence of a largely zonal circulation with dominantly western wind directions. Since the small-mammal based reconstructions indicate a seasonally homogeneous precipitation regime in large parts of the ETWZ, such an atmospheric flow could have occurred both during winter and summer. Because of the southern extension of the ETWZ, the subtropical high pressure zone (SHPZ), which is currently positioned over North Africa and the Middle East, could have been situated in a slightly more southern position than today.

The subsequent Late Miocene contraction/northward shift of the ETWZ at 9–8 Ma would imply a northward shift or expansion of the SHPZ. The study of North African fossil river systems around 8–7 Ma indeed suggests a shift from drier Tortonian to wetter Messinian conditions (Zeit Wet phase), supposedly related to the development of the African monsoon (which ultimately could be triggered by uplift of the Tibetan plateau) (Griffin, 2002). It has been proposed that the SHPZ could even have migrated as far north as the Mediterranean latitudes, creating there the appropriate conditions for the deposition of Messinian evaporites (Griffin, 2002). Although the coverage of small-

mammal localities in central Europe is poor for the Messinian, Fig. 9f suggests that this area was dry especially during this period.

Superposed on the main aridification trend in Europe there are temporary precipitation increases around 7 or 7–6 Ma, 3 Ma and possibly also at 5 Ma. (Figs. 11–13). Like the 12–9 Ma interval, also the 7–6 interval has been recognized as an interval of global cooling. 7 Ma is about the time that the West Antarctic ice sheet became a stable feature (Kennett, 1986). There is also evidence for a return to more glacial conditions in the Polar Atlantic, where accumulation of ice-rafted debris has been observed at 7.2, 6.8 and 6.3 Ma (Thiede et al., 1998). The proportion of cool-adapted neogloboquadrinids shows another rise in the Mediterranean at 7 Ma (Turco et al., 2001). Around 7 Ma, an important planktonic foraminifer cooling event occurs in the NE Atlantic (PF3, see Sierro et al., 1993) at a moment when oxygen isotope ratios show a marked rise as well (Wright et al., 1991; Hodell et al., 1994).

The precipitation increase around 3 Ma, which just precedes the onset of the late Pliocene–Pleistocene glacial–interglacial alternations, could be a reflection of the globally recognized "mid-Pliocene climatic optimum", although western Mediterranean pollen records fail to show a clear expression of this event (Fauquette et al., 1999). The effects of transgression accompanying the Pliocene optimum could explain the return to wetter conditions in eastern Europe around 3 Ma, where the Dacian Basin became re-connected to the Black Sea in the middle Romanian (Papaianopol et al., 2004). Farther continent-inward transport of Atlantic moisture as postulated by Haywood et al. (2000) could have played a role as well.

A long-term equivalent of the North Atlantic Oscillation (NAO) is an additional mechanism that should be considered in relation to late Neogene European rainfall patterns. The NAO consists of decade- to century-scale variation in position and direction of Atlantic pressure zones and westerlies (Hurrell and Van Loon, 1997). The mechanism behind these oscillations is still not well understood. During one NAO phase there will be zonal, east-oriented atmospheric flow, bringing wetter conditions in the Mediterranean, and during the opposite phase there will be or northeast-oriented flow, bringing more precipitation in central and northern Europe causing drier conditions in the Mediterranean. Recently, it has been postulated that the NAO functioned on a geological scale as well, and resulted in a (winter-) wetter Mediterranean region during late Neogene precession minima (Kloosterboer-ten Hoeve, 2000). The question whether the NAO mechanism could also contribute to the million-year precipitation fluctuations as observed here, is difficult to answer at the moment.

6.3. Gateways, remote uplift and grasslands

Closure of the Central American Seaway, which started perhaps at ~10 Ma and ended just before 4 Ma, redirected warm salty tropical ocean flows into the Gulf Stream and middle and high-latitude N Atlantic (Maier-Reimer et al., 1990). The development of the Gulf Stream could have helped in maintaining wetter (and warmer) conditions in NW Europe after 9–8 Ma (Figs. 9–12), but cannot explain aridification in other parts of the continent.

Tibetan plateau/Himalayan uplift is a better candidate for controlling the main trend of aridification as observed in the Late Miocene of Europe. Firstly, many studies point to 10–8 Ma as the age when high topographies were attained in S Asia (An et al., 2001). Secondly, atmospheric and coupled atmosphere–ocean models show that such large-scale uplift could have affected Northern Hemisphere atmospheric circulation by modifying the zonal, westerly low-level winds and causing the jet stream to meander. Westerlies over the Atlantic both weaken and take a more northeastern direction bringing more moisture and heat into northern Europe, and less moisture into southern Europe, where drier winds from a mean NE source direction increase in frequency (Broccoli and Manabe, 1997; Rind et al., 1997). In addition, the SHPZ intensifies and shifts northward (Rind et al., 1997). Northward migration of the SHPZ would offer an explanation for the small-mammal based inference (e.g. Fig. 13) that summer drying at 10–8 Ma preceded winter drying in S Europe (The boundary with the temperate zone of depressions is positioned more to the north in summer than in winter).

Grasslands could have provided an additional positive feedback with regard to the aridification process. It has been proposed that the presence of grasslands not only promotes regional drying (higher albedo, lower transpiration), but also that their large-scale expansion might have led to global cooling and mid-latitude aridification, because of the underground storage of large amounts of water and organic C (Retallack, 2000a).

7. Summary and conclusions

Fossil small-mammal communities provide valuable information on past precipitation regimes and can be

used for rainfall prediction. Present-day data from Europe show that two indices, the Invertivory Index and Arboreality Index, show significant correlations with mean annual precipitation and precipitation in the driest month. Regression equations based on these indices successfully predict the present-day rainfall gradient between the seasonally-dry Mediterranean and seasonally more homogeneous central European regimes. Underestimation of rainfall levels is to be expected in areas of orographic rainfall and along the western borders of the continent.

Predicted absolute values, trends and gradients for the late Neogene (12–3 Ma) of Europe agree very well with other estimations based on palynological, paleobotanical and large-mammal proxies. The results show that the directions of the main rainfall gradients were essentially the same as today. At 12–10 Ma the European Temperate Wet Zone (ETWZ) was a large area of 800–1200 mm rainfall per year extending from northern Spain in the west to Ukraine in the east. Precipitation levels were higher and seasonally more homogeneous than today. Between 10 and 5 Ma, the ETWZ shrinks and/or moves northward, resulting in (diachronous) aridification at intermediate latitudes (e.g. France, Hungary), whereas conditions in northern and southern areas change much less. Western Mediterranean data suggest that aridification started (10–8 Ma) in that region with the establishment of a dry (summer) season. Central Anatolia was already relatively dry (400 mm/yr) by 10 Ma, but shows an increase of precipitation at 8–7 Ma, which can also be recognized in other regions.

The maximum extension of the ETWZ at 12–10 Ma correlates temporally with a important cooling over Europe as evidenced by an increase of ice-rafted detritus in the polar Atlantic, southward migration of marine microfauna, and replacement of evergreen by deciduous vegetation elements on the continent. The penetration of large amounts of moisture far into Europe points to a largely zonal circulation with a southern position of the Subtropical High Pressure Zone (SHPZ) during this time.

The observed aridification at 9–8 Ma could best be explained by a northward extension/shifting of the SHPZ. Large-scale uplift in S Asia possibly triggered this process because of its supposed effects on both mid-latitude Atlantic atmospheric circulation and development on the Asian and African monsoon systems. Temporary increases in precipitation could be due to southward SHPZ migration associated with renewed cooling (7 Ma) or by increased advection of moisture during climatic warming (3 Ma). Uplift within Europe (e.g. Carpathians, shrinking of the Paratethys) explains further regional aridification and sharpening of gradients, especially during the Pliocene. Closure of the Central American Seaway resulted in the enhancement of the Gulf Stream and thermohaline circulation in general, and could also have contributed to the continuation of wetter conditions in NW Europe after 9–8 Ma.

Acknowledgements

I thank the EEDEN steering committee and Jordi Agustí and Oriol Oms for inviting me and organizing the second EEDEN workshop in Sabadell, November 2001. Mikael Fortelius and Torsten Utescher are thanked for reviewing the manuscript. I am grateful to Catherine Badgley, Hans de Bruijn, Gudrun Daxner-Höck, Lars van den Hoek Ostende, László Kordos, Pierre Mein, Albert van der Meulen Sevket Sen, and Engin Ünay for supplying unpublished data or material. I thank Johan van der Burgh, Johanna Kovar-Eder, Lutz Maul, Alexey Tesakov for discussions, and Mikael Fortelius and Jussi Eronen for their help and discussion at the University of Helsinki where part of this study took place. Research in Helsinki was financed by the Academy of Finland. Marjolein Boonstra is thanked for her help in preparing part of the manuscript, and Izaak Santoe for his construction of Fig. 6.

References

Abdul Aziz, H., van Dam, J.A., Hilgen, F., Krijgsman, W., 2004. Astronomical forcing in Upper Miocene continental sequences: implications for the geomagnetic polarity time scale. Earth Planet. Sci. Lett. 222, 243–258.

Adrover, R., 1986. Nuevas Faunas de Roedores en el Mio–Plioceno Continental de la Region de Teruel (España). Interes Bioestratigráfico y Paleoecologico. Instituto de Estudios Turolenses, Teruel. 423 pp.

Adrover, R., Mein, P., Moissenet, E., 1993. Roedores de la transición Mio–Plioceno de la región de Teruel. Paleoantol. Evol. 26–27, 47–84.

Aguilar, J.-P., 1982. Contribution a l'étude des micromammifères du gisement Miocène supérieur de Montredon (Hérault). 2. Les rongeurs. Palaeovertebrata 12, 81–117.

Aguilar, J.-P., Michaux, J., 1984. Le gisement à micromammifères du Mont-Hélène (Pyrénées-Orientales): apports à la connaissance de l'histoire des faunes et des environnements continentaux. Implications stratigraphiques pour le Pliocène du Sud de la France. Paléobiol. Cont. 14, 19–31.

Aguilar, J.-P., Calvet, M., Michaux, J., 1986. Description des rongeurs pliocène de la faune du Mont-Hélène (Pyrénées-Orientales, France), nouveau jalon entre les faunes de Perpignan (Serrat-d'en Vacquer) et de Sète. Palaeovertebrata 16, 127–144.

Agustí, J., 1990. The Miocene rodent succession in eastern Spain: a zoogeographical appraisal. In: Bernor, R.L., Fahlbusch, V., Mittmann, H.-W. (Eds.), The Evolution of Western Eurasian Neogene Mammal Faunas. Columbia University Press, New York, pp. 375–404.

Agustí, J., Moyà-Solà, S., Gibert, J., 1984. Mammal distribution dynamics in the eastern margin of the Iberian peninsula during the Miocene. Paléobiol. Cont. 14, 33–46.

Agustí, J., Cabrera, L., Garcés, M., Krijgsman, W., Oms, O., Parés, J. M., 2001. A calibrated mammal scale for the Neogene of western Europe; state of the art. Earth Sci. Rev. 52, 247–260.

Alcalá, L., Alonso Zarza, A.M., Álvarez Sierra, M.A., Azanza, B., Calvo, J.P., Cañaveras, J.C., van Dam, J.A., Garcés, M., Krijgsman, W., van der Meulen, A.J., Morales, J., Peláez-Campomanes, P., Pérez González, A., Sánchez Moral, S., Sancho, R., Sanz Rubio, E., 2000. El registro sedimentario y faunístico de las cuencas de Calatayud-Daroca y Teruel. Evolución paleoambiental y paleoclimática durante el Neógeno. Rev. Soc. Geol. Esp. 13, 323–343.

An, Z., Kutzbach, J.E., Prell, W.L., Porter, S.C., 2001. Evolution of Asian monsoons and phased uplift of the Himalaya-Tibetan Plateau since late Miocene times. Nature 411, 62–66.

Andrews, P., Bernor, R.L., 1999. Vicariance biogeography and paleoecology of Eurasian Miocene hominoid primates. In: Agustí, J., Rook, L., Andrews, P. (Eds.), Evolution of Neogene Terrestrial Ecosystems in Europe. Cambridge University Press, pp. 454–481.

Andrews, P., Lord, J.M., Nesbit, E.M., 1979. Patterns of ecological diversity in fossil and modern mammalian faunas. Biol. J. Linn. Soc. 11, 177–205.

Bachelet, B., 1990. Muridae and Arvicolidae (Rodentia, Mammalia) du Pliocène du sud de la France: systématique, évolution, biohcronologie. Ph.D thesis, Montpellier, 199 pp.

Bachmayer, F., Wilson, R.W., 1980. A third contribution to the fossil small mammal fauna of Kohfidisch (Burgenland), Austria. Ann. Naturhist. Mus. Wien 83, 351–386.

Bachmayer, F., Wilson, R.W., 1984. Die Kleinsäugerfauna von Götzendorf, Niederösterreich. Sitzungsber. Oesterr. Akad. Wiss. Math.-Naturwiss. Kl. 193, 303–319.

Badgley, C., Fox, D.L., 2000. Ecological biogeography of North American mammals: species density and ecological structure in relation to environmental gradients. J. Biogeogr. 27, 1437–1467.

Barrière, J., Michaux, J., 1968. Contribution à la connaissance de la stratigraphie du Pliocéne de Montpellier; étude du gisement à micromammifères de Vendargues. C. r. Somm. Séances Soc. Géol. Fr. 9, 297–299.

Bernor, R.L., 1984. A zoogeographic theater and biochronology play; the time/biofacies phenomena of Eurasian and African Miocene mammal provinces. Paléobiol. Cont. 14, 121–142.

Bernor, R.L., Kovar-Eder, J., Lipscomb, D., Rögl, F., Sen, S., Tobien, H., 1988. Systematic, stratigraphic, and paleoenvironmental contexts of first-appearing *Hipparion* in the Vienna Basin, Austria. J. Vertebr. Paleontol. 4, 427–452.

Bernor, R.L., Kordos, L., Rook, L., Agusti, J., Andrews, P., Armour-Chelu, M., Begun, D., Cameron, D.W., Damuth, J., Daxner-Höck, G., De Bonis, L., Fejfar, O., Fessaha, N., Fortelius, M., Franzen, J., Gasparik, M., Gentry, A., Heissig, K., Hernyak, G., Kaiser, T., Koufos, G.D., Krolopp, E., Janossy, D., Llenas, M., Mészáros, L., Müller, P., Renne, P., Rocek, Z., Sen, S., Scott, R., Styndlar, Z., Topal, G., Unger, P.S., Utescher, T., van Dam, J., Werdelin, L., Ziegler, R., 2003. Recent advances on multidisciplinary research at Rudabánya, late Miocene (MN9), Hungary: a compendium. Palaeontogr. Ital. 89, 3–36.

Besems, R.E., van de Weerd, A., 1983. The Neogene rodent biostratigraphy of the Teruel-Ademuz Basin (Spain). Proc. K. Ned. Acad. Wet. B86, 17–24.

Blanco, J.C., 1998. Mamíferos de España, 1, Insectívoros, Quirópteros, Primates y Carnívoros de la península Ibérica, Baleares y Canarias. Planeta, Barcelona. 457 pp.

Böhme, M., 2003. The Miocene climatic optimum; evidence from ectothermic vertebrates of central Europe. Palaeogeogr. Palaeoclimatol. Palaeoecol. 195, 389–401.

Bolliger, T., Engesser, B., Weidmann, M., 1993. Première découverte de mammifères pliocènes dans le Jura neuchâteois. Eclogae Geol. Helv. 86, 1031–1068.

Broccoli, A.J., Manabe, S., 1997. Tectonic uplift and climate change. In: Ruddiman (Ed.), Tectonic Uplift and Climate Change. Plenum Press, New York, pp. 89–121.

Bruch, A.A., Utescher, T., Mosbrugger, V., Gabrielyan, L., Ivanov, D. A., 2006. Late Miocene climate in the circum-Alpine realm—a quantitative analysis of terrestrial palaeofloras. Palaeogeogr. Palaeoclimatol. Palaeoecol. 238, 270–280.

Churchfield, S., 1990. The Natural History of Shrews. Cornell University press, Ithaca, New York. 178 pp.

Crochet, J.-Y., 1986. Insectivores pliocènes du sud de la France (Languedoc-Roussillon) et du nort-est de l'Espagne. Palaeovertebrata 16, 145–171.

Crochet, J.-Y., Green, M., 1982. Contribution a l'étude des micromammifères du gisement Miocène supérieur de Montredon (Hérault). 3. Les insectivores. Palaeovertebrata 12, 119–131.

Crowley, T.J., 1996. Pliocene climates; the nature of the problem. Mar. Micropaleontol. 27, 3–12.

Crowley, T.J., North, G.R., 1991. Paleoclimatology. Oxford University Press, New York.

Daams, R., Freudenthal, M., van der Meulen, A.J., 1988. Ecostratigraphy of micromammal faunas from the Neogene of the Calatayud–Teruel Basin. Scr. Geol., Spec. Issue 1, 287–302.

Daams, R., van der Meulen, A.J., Álvarez Sierra, M., Peláez-Campomanes, P., Calvo, J.P., Alonso Zarza, A., Krijgsman, W., 1999. Stratigraphy and sedimentology of the Aragonian (Early to Middle Miocene) in its type area (North–Central Spain). Newsl. Stratigr. 37, 103–139.

Dahlmann, T., 2001. Die Kleinsäuger der unter-pliozänen Fundstelle Wölfersheim in der Wetterau (Mammalia: Lipotyphla Chiroptera, Rodentia). Cour. Forschungsinst. Senckenberg 227, 1–129.

Damuth, J., 1992. Taxon-free characterization of animal communities. In: Behrensmeyer, A.K., Damuth, J., DiMichele, W., Potts, R., Sues, H.D., Wing, S. (Eds.), Terrestrial Ecosystems Through Time. University of Chicago Press, Chicago, pp. 183–203.

Damuth, J., 1999. Habitat and Climate Inference from the Structure of Mammal Communities. Research Projects. National Center for Ecological Analysis and Synthesis http://www.nceas.ucsb.edu.

Damuth, J., Fortelius, M., 2001. Reconstructing mean annual precipitation, based on mammalian dental morphology and local species richness. In: Agustí, J., Oms, O. (Eds.), Late Miocene to Early Pliocene Environments and Ecosystems, Abstracts of the 2nd EEDEN Workshop, Sabadell, pp. 23–24.

Damuth, J., van Dam, J.A., Utescher, T., 2003. Palaeoclimate proxies from biotic proxies. Pp 23–25. In: Bernor, R.L., Kordos, L., Rook, L., et al. (Eds.), Recent Advances on Multidisciplinary Research at Rudabánya, Late Miocene (MN9), Hungary: A Compendium. Palaeontographica Italica, vol. 89, pp. 1–34.

Daxner-Höck, G., 1980. Rodentia (Mammalia) des Eichkogels bei Mödling (Niederösterreich). Ann. Naturhist. Mus. Wien 83, 135–152.

de Bruijn, H., 1976. Vallesian and Turolian rodents from Biota, Attica and Rhodes (Greece). Proc. K. Ned. Akad. Wet., B 79, 361–384.

de Bruijn, H., 1989. Smaller mammals from the Upper Miocene and Lower Pliocene of the Strimon Basin, Greece: Part 1. Rodentia and Lagomorpha. Boll. Soc. Paleontol. Ital. 28, 189–195.

de Bruijn, H., 1997. Vertebrates from the Early Miocene lignite deposits of the opencast mine Oberdorf (Western Styrian Basin, Austria). 6. Rodentia 1 (Mammalia). Ann. Nat.hist. Mus. Wien, Ser. A Mineral. Petrogr. Geol. Paläontol. Anthropol. Prähist. 99, 99–137.

de Bruijn, H., Daams, R., Daxner-Höck, G., Fahlbusch, V., Ginsburg, L., Mein, P., Morales, J., 1992. Report of the RCMNS working group on fossil mammals, Reisensburg 1990. Newsl. Stratigr. 26, 65–118.

de Bruijn, H., Saraç, G., van den Hoek Ostende, L.W., Roussiakis, S., 1999. The status of the genus name *Parapodemus* Schaub, 1938; new data bearing on an old controversy. Deinsia 7, 95–112.

de Giuli, C., 1989. The rodents of the Brisighella latest Miocene fauna. Boll. Soc. Paleont. Ital. 28, 197–212.

de Jong, F., 1988. Insectivora from the upper Aragonian and the lower Vallesian of the Daroca–Villafeliche area in the Calatayud–Teruel Basin (Spain). Scr. Geol., Spec. Issues 1, 253–285.

Engesser, B., 1972. Die obermiozäne Säugetier Fauna von Anwil (Baselland). Tätigk.ber. Nat.forsch. Ges. Baselland 28, 37–363.

Engesser, B., 1980. Insectivore und Chiroptera (Mammalia) aus dem Neogen der Türkei. Paläontol. Abhandlungen 102, 47–149.

Engesser, B., 1989. The Late Tertiary small mammals of the Maremma region (Tuscany, Italy): 2nd part. Muridae and Cricetidae (Rodentia Mammalia). Boll. Soc. Paleontol. Ital. 28, 227–252.

Engesser, B., 1999. Family Eomyidae. In: Rössner, G.E., Heissig, K. (Eds.), The Miocene Land Mammals of Europe. Pfeil, München, pp. 319–335.

Fahlbusch, V., Mayr, H., 1975. Eine unterpliozäne Kleinsäugerfauna aus der Oberen Süsswasser-Molasse Bayerns. Mitt. Bayer. Staatsslg. Paläont. Hist. Geol. 15, 91–111.

Farjanel, G., Mein, P., 1984. Une association de mammifères et de pollens dans la formation continentale des "Marnes de Bresse" d'âge Miocène supérieur, à Ambérieu. Géol. Fr. 1–2, 131–148.

Fauquette, S., Guiot, J., Suc, J.-P., 1998. A method for climatic reconstruction of the Mediterranean Pliocene using pollen data. Palaeogeogr. Palaeoclimatol. Palaeoecol. 144, 183–201.

Fauquette, S., Suc, J.-P., Guiot, J., Diniz, F., Feddi, N., Zheng, Z., Bessais, E., Drivaliari, A., 1999. Climate and biomes in the West Mediterranean area during the Pliocene. Palaeogeogr. Palaeoclimatol. Palaeoecol. 152, 15–36.

Fejfar, O., 1990. The Neogene VP sites of Czechoslovakia: a contribution to the Neogene terrestric biostratigraphy of Europe based on rodents. In: Bernor, R.L., Fahlbusch, V., Mittmann, H.-W. (Eds.), The Evolution of Western Eurasian Neogene Mammal Faunas. Columbia University Press, New York, pp. 211–236.

Fortelius, M., Hokkanen, A., 2001. The trophic context of hominoid occurrence in the later Miocene of western Eurasia — a primate-free view. In: de Bonis, L., Koufos, G., Andrews, P. (Eds.), A Phylogeny of the Neogene Hominoid Primates of Eurasia. Cambridge University Press, Cambridge, pp. 19–47.

Fortelius, M., Werdelin, L., Andrews, P., Bernor, R.L., Gentry, A., Humphrey, L., Mittmann, H.-W., Viranta, S., 1996. Provinciality, diversity, turnover and paleoecology in land mammal faunas of the later Miocene of western Eurasia. In: Bernor, R.L., Fahlbusch, V., Mittmann, H.-W. (Eds.), The Evolution of Western Eurasian Neogene Mammal Faunas. Columbia University Press, New York, pp. 414–448.

Fortelius, M., Eronen, J., Jernvall, J., Liu, L., Pushkina, D., Rinne, J., Tesakov, A., Vislobokova, I., Zhang, Z., 2002. Fossil mammals resolve regional patterns of Eurasian climate change during 20 million years. Evol. Ecol. Res. 4, 1005–1016.

Forteliusl, M., Eronen, J., Liu, L., Pushkina, D., Tesakov, A., Vislobokova, I., Zhang, Z., 2006. Late Miocene and Pliocene large land mammals and climatic changes in Eurasia. Palaeogeogr. Palaeoclimatol. Palaeoecol. 238, 219–227.

Frakes, L.A., Francis, J.E., Syktus, J.I., 1992. Climate Modes of the Phanerozoic. Cambridge University Press, Cambridge.

Franzen, J.L., Storch, G., 1999. Late Miocene mammals from central Europe. In: Agustí, J., Rook, L., Andrews, P. (Eds.), Evolution of Neogene Terrestrial Ecosystems in Europe. Cambridge University Press, pp. 165–190.

Freudenthal, M., Kordos, L., 1989. *Cricetus polgardiensis* sp. nov. and *Cricetus kormosi* Schaub, 1930 from the Late Miocene Polgárdi localities (Hungary). Scr. Geol. 89, 71–100.

Gibert, J.G., 1975. Distribución bioestratigráfica de los insectívoros del Mioceno en al NE. de España. Biotopos, comparación de cuencas y localidades. Relaciones faunísticas con América del Norte. Acta Geol. Hisp. 5, 167–169.

Griffin, D.L., 2002. Aridity and humidity; two aspects of the late Miocene climate of North Africa and the Mediterranean. Palaeogeogr. Palaeoclimatol. Palaeoecol. 182, 65–91.

Haywood, A.M., Sellwood, B.W., Valdes, P.J., 2000. Regional warming; Pliocene (3 Ma) paleoclimate of Europe and the Mediterreanean. Geology 28, 1063–1066.

Heizmann, E.P.J., Reiff, W., 2002. De Steinheimer Meteorkrater. Verlag Freidrich Pfeil, München.

Hershkovitz, P., 1997. Dynamics of rodent molar evolution: a study based on new world Cricetinae, family Muridae. J. Dent. Res. 5, 829–842 (Supplement to No.).

Hodell, D.A., Benson, R.H., Kent, D.V., Boersma, A., Rakic-El Bied, K., 1994. Magnetostratigraphic, biostratigraphic, and stable isotope stratigraphy of an Upper Miocene drill core from the Salé Briqueterie (northwestern Morocco): a high-resolution chronology for the Messinian stage. Paleoceanography 9, 835–855.

Hurrell, J.W., Van Loon, H., 1997. Decadal variations in climate associated with the North Atlantic oscillation. Clim. Change 36, 301–326.

Hürzeler, J., Engesser, B., 1976. Les faunes de mammifères néogènes de Baccin de Baccinello (Grosseto, Italie). C. R. Acad. Sc., Sér. D 283, 333–336.

Ivanov, D., Ashraf, A.R., Mosbrugger, V., Palamarev, E., 2002. Palynological evidence for Miocene climate change in the Forecarpathian Basin (central Paratethys, NW Bulgaria). Palaeogeogr. Palaeoclimatol. Palaeoecol. 178, 9–37.

Jánossy, D., 1986. Pleistocene Vertebrate Faunas of Hungary. Elsevier, Amsterdam. 208 pp.

Jones, R.W, Simmons, M.D., 1997. A review of the stratigraphy of eastern Paratethys (Oligocene–Holocene), with particular emphasis on the Black Sea. In: Robinson, A.G. (Ed.), Regional and Petroleum Geology of the Black Sea and Surrounding Region. AAPG Memoir, vol. 68, pp. 39–51.

Kälin, D., Engesser, B., 2001. Die jungmiozäne Säugetierfauna vom Nebelbergweg bei Nunningen (Kanton Solothurn, Schweiz). Schweiz. Paläontol. Abh. 121, 4–61.

Kay, R.F., Madden, R.H., 1997. Mammals and rainfall: paleoecology of the middle Miocene at La Venta (Colombia, South America). J. Hum. Evol. 32, 161–199.

Kennett, J.P., 1986. Miocene to early Pliocene oxygen and carbon isotope stratigraphy in the southwest Pacific, Deep Sea Drilling Project Leg 90. Initial Rep. Deep Sea Drill. Proj. 90, 1383–1411.

Kloosterboer-ten Hoeve, M., 2000. Cyclic changes in the late Neogene vegetation of northern Greece. LPP Contrib. Ser. 12, 1–131.

KNMI, 1997. Wereld Klimaat Informatie http://www.knmi.nl.

KNMI, 1998. Wereld Klimaat Informatie (WKI). http://www.knmi.nl.

Köhler, M., 1993. Skeleton and habitat of Recent and fossil ruminants. Münch. Geowiss.Abh., A, Geol. Paläontol. 25, 5–88.

Kordos, L., 1987. *Karstocricetus skofleki* gen. n., sp. n. and the evolution of the Late Neogene Cricetidae in the Carpathian Basin. Fragm. Mineral. Palaeontol. 13, 65–88.

Kovar-Eder, J., 2003. Vegetation dynamics in Europe during the Neogene. Deinsia 10, 373–391.

Kowalski, K., 1990. Stratigraphy of Neogene mammals of Poland. In: Bernor, R.L., Fahlbusch, V., Mittmann, H.-W. (Eds.), The Evolution of Western Eurasian Neogene Mammal Faunas. Columbia University Press, New York, pp. 193–209.

Kretzoi, M., 1951. A csákvári *Hipparion*-fauna. Földt. Közlöny 81, 384–401.

Kretzoi, M., 1984. A Sümeg-gerinci fauna és faunaszakasz. Geol. Hung., Ser. Geol. 20, 214–222.

López Martínez, N., Sesé, C., Sanz, J.L., 1977. La microfauna (Rodentia, Insectivora, Lagomorpha y Reptilia) de als fisuras del Mioceno medio y superior del escobosa de Calatañazor (Soria, España). Trabajos N/Q 8, 47–73.

Lunkka, J.P., Fortelius, M., Kappelman, J., Sev, S., 1999. Chronology and mammal faunas of the Miocene Sinap Formation, Turkey. In: Agustí, J., Rook, L., Andrews, P. (Eds.), Evolution of Neogene Terrestrial Ecosystems in Europe. Cambridge University Press, pp. 238–272.

Mai, D.H., 1995. Tertiäre Vegetationsgeschichte Europas. Gustav Fischer, Jena. 691 pp.

Maier-Reimer, E., Mikolajewicz, U., Crowley, T.-J., 1990. Ocean general circulation model sensitivity experiment with an open Central American isthmus. Paleoceanography 5, 349–366.

Martín-Suárez, E., Oms, O., Freudenthal, M., Agustí, J., Parés, J.M., 1998. Continental Mio–Pliocene transition in the Granada Basin. Lethaia 31, 161–166.

Mein, P., 1999. The small mammal Vallesian and Turolian succession of France. In: Agustí, J., Rook, L., Andrews, P. (Eds.), Evolution of Neogene Terrestrial Ecosystems in Europe. Cambridge University Press, pp. 140–164.

Mein, P., Adrover, R., 1977. Yacimiento de El Arquillo III, en Teruel, España (Nota preliminar). Acta Geol. Hisp. 12, 46–48.

Mein, P., Moissenet, E., Adrover, R., 1990. Biostratigraphie du Néogène supérieur de Teruel. Paleontol. Evolució 23, 121–139.

Mészáros, L.G., 1996. Soricidae (Mammalia, Insectivora) remains from three Late Miocene localities in western Europe. Ann. Univ. Sci. Bp., Sect. Geol. 31 (5–25), 119–122.

Mészáros, L.G., 1998. Late Miocene Soricidae (Mammalia) fauna from Tardosbánya (Western Hungary). Hantkeniana 2, 103–125.

Mészáros, L.G., 1999. An exceptionally rich Soricidae (Mammalia) fauna from the upper Miocene localities of Polgárdi (Hungary). Ann. Univ. Sci. Bp., Sect. Geol. 32, 5–34.

Michaux, J., 1969. Les gisements de vertébrés de la région montpelliéraine. 3. Gisements pliocènes. Bull. Bur. Rech. Géol. Min. 2, 31–37.

Mitchell-Jones, A.J., Amori, G., Bogdanowicz, W., Kryštufek, B., Reijnders, P.J.H., Spitzenberger, F., Stubbe, M., Thissen, J.B.M., Vohralík, V., Zima, J., 1999. The Atlas of European Mammals. Poyser Natural History, London.

Montoya, P., 1994. Los macromamíferos del Mioceneo superior del área de Crevillente (Alicante). Tesis Doctoral, Universitat de València, 421 pp.

Montoya, P., 1997. Los yacimientos con mamíferos Neógenos de la comunidad Valenciana. Cidaris 11–12, 24–47.

Mörs, Th., Von Koenigswald, W., Von Der Hoch, F., 1998. Rodents Mammalia from the late Pliocene Reuver Clay of Hambach (Lower Rhine Embayment, Germany). Meded. - Ned. Inst. Toegepaste Geowet. TNO 60, 135–159.

Mosbrugger, V., Utescher, T., 1997. The coexistence approach; a method for quantitative reconstructions of Tertiary terrestrial palaeoclimate data using plant fossils. Palaeogeogr. Palaeoclimatol. Palaeoecol. 134, 61–86.

Mudie, P.J., Helgason, J., 1983. Palynological evidence for Miocene climatic cooling in eastern Iceland about 9.8 Myr ago. Nature 303, 689–692.

Müller, M., 1996. Handbuch ausgewählter Klimastationen der Erde. Gerold Richter, Trier.

Nadachowski, A., 1990. Review of fossil Rodentia from Poland. Senckenberg. Biol. 70, 229–250.

Nadachowski, A., 2001. New important Neogene and Pleistocene mammal assemblages from Poland. Boll. Soc. Paleontol. Ital. 40, 243–248.

Nesin, V., Nadachowski, A., 2001. Late Miocene and Pliocene small mammal faunas (Insectivora, Lagomorpha, Rodentia) of south-eastern Europe. Acta Zool. Cracov. 44, 107–135.

Nicholson, S., Flohn, H., 1980. African environmental and climatic changes and the general circulation in late Pleistocene and Holocene. Clim. Change 2, 313–348.

Niethammer, J., Krapp, F., 1978. Handbuch der Säugetiere Europas. Akademische Verlagsgesellschaft, Wiesbaden.

Nowak, R.M., 1991. Walker's Mammals of the World. John Hopkins University Press, Baltimore.

Opdyke, N., Mein, P., Lindsay, E., Perez-Gonzales, A., Moissenet, E., Norton, V.L., 1997. Continental deposits, magnetostratigraphy and vertebrate paleontology, late Neogene of eastern Spain. Palaeogeogr. Palaeoclimatol. Palaeoecol. 133, 129–148.

Papaianopol, I., Marinescu, Fl., Marunteanu, M., Krstic, N., Macaleþ, R., 2004. Neogen der Zentralen Paratethys. Pliozän Pl_2, Romanian. Chronostratigraphie und Neostratotypen 10. Rumänische Akademie, Bukarest.

Parrish, J.T., Ziegler, A.M., Scotese, C.R., 1982. Rainfall patterns and the distribution of coals and evaporites in the Mesozoic and Cenozoic. Palaeogeogr. Palaeoclimatol. Palaeoecol. 40, 67–101.

Pérez, B., Soria, D., 1990. Análisis de las comunidades de mamíferos del Plioceno de Layna (Soria) y La Calera (Teruel). Paleontol. Evol. 23, 231–238.

Pérez Vila, M.-J., Fauquette, S., Suc, J.-P., Bessedik, M., 2001. Palynological contribution to estimation of Mio–Pliocene altitude of eastern Pyrenees. In: Agustí, J., Oms, O. (Eds.), Late Miocene to Early Pliocene Environments and Ecosystems, Abstracts of the 2nd EEDEN Workshop, Sabadell, pp. 52–53.

Pevzner, M.A., Vangengeim, E.A., Vislobokova, I.A., Sotnikova, M. V., Tesakov, A.S., 1996. Ruscinian of the territory of the former Soviet Union. Newsl. Stratigr. 33, 77–97.

Potts, R., Behrensmeyer, A.K., 1992. Late Cenozoic terrestrial ecosystems. In: Behrensmeyer, A.K., Damuth, J., DiMichele,

W., Potts, R., Sues, H.D., Wing, S. (Eds.), Terrestrial Ecosystems Through Time. University of Chicago Press, Chicago, pp. 419–541.

Quade, J.T., Solounias, N., Cerling, T.E., 1994. Stable isotope evidence from paleosol carbonates and fossil teeth in Greece for forest or woodlands over the past 11 Ma. Palaeogeogr. Palaeoclimatol. Palaeoecol. 108, 41–53.

Rabeder, G., 1970. Die Wirbeltierfauna aus dem Alt-Pliozaen (O-Pannon) vom Eichkogel bei Moedling (NOe.); I, Allgemeines; II, Insectivora. Ann. Naturhist. Mus. Wien 74, 589–595.

Radulescu, C., Samson, P.M., Petculescu, A., 2000. Les environnements du Pliocène inferieur et moyen du Bassin Dacique; mise en parallele climatique entre les micromammiféres et les palynoflores. Acta Palaeontol. Rom. 2, 427–432.

Retallack, G.J., 2000a. Cenozoic expansion of grasslands and climatic cooling. J. Geol. 109, 407–426.

Retallack, G.J., 2000b. Depth to pedogenic carbonate horizon as a paleoprecipitation indicator? Comment. Geology 28, 572.

Reumer, J.W.F., 1985. The paleoecology of Soricidae (Insectivora, Mammalia) and its application to the debate on the Plio–Pleistocene boundary. Rev. Paléobiol. 4, 211–214.

Rind, D., Russell, G., Ruddiman, W.F., 1997. The effects of uplift on ocean–atmosphere circulation. Tectonic uplift and climate change. In: Ruddiman (Ed.), Tectonic Uplift and Climate Change. Plenum Press, New York, pp. 123–147.

Rivas-Carballo, M.R., 1991. The development of vegetation and climate during the Miocene in the south-eastern sector of the Duero Basin (Spain). Rev. Palaeobot. Palynol. 67, 341–351.

Rögl, F., Zapfe, H., Bernor, R.L., Brzobohaty, R., Daxner-Höck, G., Draxler, I., Feyfar, O., Gaudant, J., Herrmann, P., Rabeder, G., Schultz, O., Zetter, R., 1993. Die Primatenfundstelle Götzendorf an der Leitha, Niedreösterreich (Obermiozän des Wiener beckens. Jb. Geol. B.-A. 136, 503–526.

Ruddiman, W., Raymo, M., Prell, W., Kutzbach, J., 1997. The uplift-climate connection; a synthesis. In: Ruddiman (Ed.), Tectonic Uplift and Climate Change. Plenum Press, New York, pp. 471–515.

Ruis Bustos, A., 2002. Características climáticas y estratigráficas de los sedimentos continentales de la Cordillera Bética durante el Plioceno, a partir de las faunas de mamíferos. Pliocénica 2, 44–64.

Sabol, M., 2001. Villafranchian locality Hajnáèka 1: comparison of older data with new ones. Slovak Geol. Mag. 7, 275–287.

Schmidt-Kittler, N., de Bruijn, H., Doukas, C., 1995. The vertebrate locality Maramena (Macedonia, Greece) at the Turolian–Ruscinian boundary. Münch. Geowiss. Abh., A Geol. Paläontol. 28, 9–18.

Sen, S., Bouvrain, G., Geraads, D., 1998. Pliocene vertebrate locality of Calta, Ankara, Turkey; 12, Paleoecology, biogeography and biochronology. Geodiversitas 20, 497–510.

Sesé, C., 1989. Micromamíferos del Mioceno, Plioceno y Pleistoceno de la cuenca de Guadix-Baza (Granada). In: Alberdi, M.T., Bonadona, F.P. (Eds.), Geología y Paleontología de la Cuenca de Guadix-Baza. Museo Nacional de Ciencas Naturales, CSIC, Madrid, pp. 13–51.

Shatilova, I., Ramishvili, I., 1984. Climate and flora of the Neogene of Western Georgia (USSR). Paléobiol. Cont. 14, 423–432.

Sickenberg, O., Becker-Platen, J.D., Benda, L., Berg, D., Engesser, B., Gaziry, W., Heissig, K., Huenermann, K.A., Sondaar, P.Y., Schmidt-Kittler, N., Staesche, U., Steffens, P., Tobien, H., 1975. Die Gliederung des höheren Jungtertiärs und Altquartärs in der Türkei nach Vertebraten und ihre Bedeutung für die internationale Neogen-Stratigraphie. Geol. Jahrb., B 15, 1–67.

Sierro, F.J., Flores, J.A., Civis, J., Gonzáles Delgado, J.A., Francés, G., 1993. Late Miocene globorotaliid event-stratigraphy and biogeography in the NE-Atlantic and Mediterranean. Mar. Micropaleontol. 21, 143–168.

Singh, G., 1988. History of aridland vegetation and climate — a global perspective. Biol. Rev. 63, 159–195.

Solounias, N., Plavcan, J.M., Quade, J., Witmer, L., 1999. The paleoecology of the Pikermiam Biome and the sacanna myth. In: Agustí, J., Rook, L., Andrews, P. (Eds.), Evolution of Neogene Terrestrial Ecosystems in Europe. Cambridge University Press, pp. 436–453.

Storch, G., Dahlmann, T., 2000. *Desmanella rietscheli*, ein neuer Talpide aus dem Obermiozän von Dorn-Dürkheim 1, Rheinhessen (Mammalia, Lipotyphla). Carolinea 28, 65–69.

Storch, G., Engesser, B., Wuttke, M., 1996. Oldest fossil record of gliding in rodents. Nature 379, 439–441.

Suc, J.-P., Bessais, E., 1990. Pérennité d'un climat thermoxérique en Sicile, avant, pendant et après la crise de salinité´ messinienne. C. R. Acad. Sci. Paris 310 (ser. II), 1701–1707.

Suc, J.-P., Diniz, F., Leroy, S., Poumot, C., Bertini, A., Dupont, L., Clet, M., Bessais, Zheng, Z., Fauquette, S., Ferrier, J., 1995. Zanclean (~Brunssumian) to early Piazencian (~early–middle Reuverian) climate from 4° to 54° north latitude (West Africa, West Europe and West Mediterranean. Meded. Rijks Geol. Dienst 52, 43–56.

Suc, J.-P., Fauquette, S., Suc, Bessedik, M., Bertini, A., Zheng, Z., Clauzon, G., Suballyova, D., Diniz, F., Quézel, P., Feddi, N., J.-P., Clet, M., Bessais, E., Bachiri Taoufiq, N., Méon, H., Cobourieu-Nebout, N., 1999. Neogene vegetation changes in West European and West circum-Mediterranean areas. In: Agustí, J., Rook, L., Andrews, P. (Eds.), Evolution of Neogene Terrestrial Ecosystems in Europe. Cambridge University Press, pp. 378–388.

Sümengen, M., Ünay, E., Saraç, de Bruijn, H., Terlemez, I., Gürbüz, M., 1989. New Neogene rodent assemblages from Anatolia (Turkey). In: Bernor, R.L., Fahlbusch, V., Mittmann, H.-W. (Eds.), The Evolution of Western Eurasian Neogene Mammal Faunas. Columbia University Press, New York, pp. 61–72.

Svelitskaya, T.V., 1999. The main stages of environmental evolution in the northern Black Sea coastal region during the Pliocene. In: Wrenn, J.H., Suc, J.-P., Leroy, S.A.G. (Eds.), The Pliocene: Time of Change; American Association of Stratigraphic Palynologists Foundation, pp. 173–177.

Tesakov, A.S., 1998. Voles of the Tegelen fauna. Meded. - Ned. Inst. Toegepaste Geowet. TNO 60, 71–134.

Thiede, J., Winkler, A., Wolf-Welling, T., Eldholm, O., Myhre, A.M., Baumann, K.-H., Heinrich, R., Stein, R., 1998. Late Cenozoic history of the polar North Atlantic; results from ocean drilling. Quat. Sci. Rev. 17, 185–208.

Thompson, R.S., Fleming, R.F., 1996. Middle Pliocene vegetation; reconstructions, paleoclimatic inferences, and boundary conditions for climate modeling. Mar. Micropaleontol. 27, 27–49.

Traverse, A., 1982. Response of world vegetation to Neogene tectonic and climatic events. Alcheringa 6, 197–209.

Turco, E., Hilgen, F.J., Lourens, L.J., Shackleton, N.J., Zachariasse, W. J., 2001. Punctuated evolution of global climate cooling during the late Middle to early Late Miocene: high-resolution planktonic foraminiferal and oxygen isotope records from the Mediterranean. Paleoceanography 16, 405–423.

Ünay, E., 1981. Middle and upper Miocene rodents from the Bayraktepe section (Canakkale, Turkey). Proc. K. Ned. Akad. Wet., Ser. B Phys. sci. 84, 217–238.

Utescher, T., Mosbrugger, V., Ashraf, A.R., 2000. Climate evolution in northwest Germany over the last 25 million years. Palaios 15, 430–449.

van Dam, J.A., 1997. The small mammals from the upper Miocene of the Teruel–Alfambra region (Spain): paleobiology and paleoclimatic reconstructions. Geol. Ultraiectina 156, 1–204.

van Dam, J.A., Weltje, G.J., 1999. Reconstruction of the late Miocene climate of Spain using rodent paleocommunity successions: an application of end-member modelling. Palaeogeogr. Palaeoclimatol. Palaeoecol. 151, 267–305.

van Dam, J.A., Alcalá, L., Alonso Zarza, A.M., Calvo, J.P., Garcés, M., Krijgsman, W., 2001. The Upper Miocene mammal record from the Teruel–Alfambra region (Spain): the MN system and continental stage/age concepts discussed. J. Vertebr. Paleontol. 21, 367–385.

van der Burgh, J., 1987. Miocene floras in the Lower Rhenish Basin and their ecological interpretation. Rev. Palaeobot. Palynol. 52, 299–366.

van der Meulen, A.J., Daams, R., 1992. Evolution of Early–Middle Miocene rodent faunas in relation to long-term palaeoenvironmental changes. Palaeogeogr. Palaeoclimatol. Palaeoecol. 93, 227–253.

van der Meulen, A.J., de Bruijn, H., 1982. The mammals from the Lower Miocene of Aliveri (Island of Evia, Greece): Part 2. The Gliridae. Proc. K. Ned. Acad. Wet., B 85, 485–524.

van der Meulen, A.J., van Kolfschoten, T., 1986. Review of the late Turolian to early Biharian mammal faunas from Greece and Turkey. Mem. Soc. Geol. Ital. 31, 201–211.

van de Weerd, A., 1976. Rodent faunas of the Mio–Pliocene continental sediments of the Teruel–Alfambra region, Spain. Utrecht Micropaleontol. Bull., Spec. Publ. 2, 1–217.

Wright, J.D., Miller, K.G., Fairbanks, R.G., 1991. Evolution of modern deepwater circulation: evidence from the late Miocene Southern Ocean. Paleoceanography 6, 275–290.

Zachos, J., Pagani, M., Sloan, L., Thomas, E., Billups, K., 2001. Trends, rhythms, and aberrations in global climate 65 Ma to present. Science 292, 686–693.